PREPARATION OF A NON-EVAPORATING CONTACT ANGLE STANDARD

REFERENCE MATERIAL

_____

A Thesis

Presented to

The Faculty of the Department of Chemistry

Sam Houston State University

_____

In Partial Fulfillment

of the Requirements for the Degree of

Master of Science

_____

by

Trisha M. O'Bryon

August, 2012

PREPARATION OF A NON-EVAPORATING CONTACT ANGLE STANDARD

REFERENCE MATERIAL

by

Trisha M. O'Bryon

_____

APPROVED:

_____
Dr. Darren Williams
Thesis Director

_____
Dr. Richard Norman

_____
Dr. David Thompson

Approved:

_____
Dr. Jerry Cook, Interim Dean
College of Science

DEDICATION

I would like to dedicate this to my family. Without their continual support and guidance I never would have been able to become the chemist I am today. Thank you to my mother for your unwillingness to let me fall short of my potential and your ability to always be there to lend an open mind and heart. Thank you to my father, who without your level head and humor I would have never learned to laugh at myself and learn from the mistakes. And finally, thank you to my brother for your continued support and encouragement.

I appreciate all that you have done, especially those that have ever taught me in class or life. You have helped make me a better person and a better chemist and I know that could never have achieved this without you. Thank you.

ABSTRACT

O'Bryon, Trisha M., *Preparation of a non-evaporating contact angle standard reference material*. Master of Science (Chemistry), August, 2012, Sam Houston State University, Huntsville, Texas.

Purpose

The purpose of this project was to combine previous contact angle measurement methods with improvements in digital imaging and computing to develop a standard method and reference material for calculating contact angle and therefore surface energy. Modernization of these methods and the development of this standard provide a low cost and effective way to collect and analyze data for use in the paints, cleaning and adhesives industries, to name a few.

Methods

Current contact angle methods were divided into three major categories, specifically the side-on, top-down and reflected angle methods. In order to compare the validity of each of the methods, a solid, non-evaporating standard needed to be created. The three standards investigated were a ruby ball, a steel ball, and a piece of pressed aluminum. Each were mounted in such a way as to mimic a sessile drop with a contact angle of less than or greater than 90 degrees.

Findings

The side-on method using the digital microscope with the contact angle measured using the Manual Points Procedure was defined as the lab accepted standard as it most closely matches the current industry instruments like the goniometer. After determining the accepted angle for the proposed standards, the reflected side-on method, top-down and reflected angle methods were analyzed the standards and compared to the accepted

angles for all of the standards. In the end, the steel ball was the preferred standard as it was well machined and could mimic contact angles of less than and greater than 90 degrees simply by changing its mount.

The applications for this type of standard are nearly limitless. The mounts and standards are inexpensive, effective ways of determining contact angles. The use of a contact angle standard can be used to verify techniques and train technicians. By using a non-evaporating standard, a variety of liquids with an array of surfaces can be tested and analyzed. The non-evaporating contact angle standard fills an important void in the coating and adhesive industry.

KEY WORDS: contact angle, contact angle standard, surface energy, volume of a spherical cap

ACKNOWLEDGEMENTS

TABLE OF CONTENTS

LIST OF TABLES

LIST OF FIGURES

CHAPTER I

INTRODUCTION

Surface wettability and surface energy have been used in various industries to explore surface coating adhesion and surface cleanliness. In an attempt to understand these characteristics, the contact angle of a liquid on a surface may be measured to give wettability and surface energy information. Since Young's first description of contact angles [1] in 1805, many have adapted his description and generated methods capable of measuring contact angles. Barth [2] measures the dynamic contact angle of a coating liquid while Sutton [3-4] uses capillary pressure. Blitshteyn [5], Friedrich [6], and Wright [7] project an image of the droplet so that the contact angle can be measured off the projection. Dumoulin [8], Martin [9], and Schneider [10] use reflected light or a laser beam to measure the contact angle. Poppe [11] uses a goniometer and Wapner [12] even uses folding metal plates to analyze the change of a droplet from wetting to non-wetting behavior. Many of these are primitive, but those developed by Irving Langmuir [13-14] and J. J. Bikerman [15] may be combined with the improvements in digital imaging and computing to bring a contact angle measurement to the modern coating or adhesive production facility.

In measuring the surface energy of a solid it is important to note that the results can vary greatly upon the choice of liquid and technique. Therefore, an attempt must be made to create a physical standard and method that can determine the surface energy of any surface. To reliably implement a standard contact angle technique, a solid standard reference material must be created which cannot be affected by environmental changes and has a known contact angle. By using a contact angle standard, any measurement

technique, when preformed correctly, will produce a value that can be compared to the known angle. The standard is the best way to characterize human and mechanical uncertainty among labs or companies. This thesis describes the development and evaluation of the standard reference material and analysis procedure.

The National Institute of Standards and Technology currently has not defined a contact angle standard. The American Society for Testing and Materials has developed many standard procedures relating to measuring the contact angle of a sessile drop[16-17] but a calibration standard is not adequately defined which makes it impractical to discuss the accuracy of measurements between methods or between labs. By creating a well-defined and characterized calibration standard, this project fills that void.

In developing this standard, three methods of measuring contact angle were compared; the side-on method as defined by Young, the top-down method as defined by Bikerman, and the reflected angle method as defined by Langmuir. Each method presents its own unique challenges and advantages. The standards explored include a ruby ball, pressed aluminum, and a steel ball all mounted differently and used in combination with one or more of the measurement methods.

CHAPTER II

CONTACT ANGLE THEORY

Surface energy and surface tension are the two primary components in determining the characteristics of a solid-liquid interaction. The surface energy of a solid is the amount of energy required to create a certain area of surface, measured in Joules per meter squared [18]. The energy is measured indirectly using wetting behavior of test liquids with known surface tensions. Surface tension is the surface energy of a liquid that it is expressed as a force in one dimension measured in newtons per meter [18]. Mathematically, the surface tension γ_{23} is defined as the force vector between the liquid (*2*) and gas (*3*) phases of a drop. By multiplying the surface tension by meters over meters, thus giving a surface area, the surface energy can be measured in joules per meter. Equation 1 describes the mathematical relationship.

$$\gamma_{23} = \frac{N}{m} \cdot \frac{m}{m} = \frac{J}{m^2} \tag{1}$$

Zisman Plot

In industry, a Zisman plot is used to examine the relationship between the surface tension of a liquid and the surface energy of a solid surface. W. A. Zisman developed a standard technique to determine the surface energy of a smooth, planar surface by studying the contact angle behavior of probe liquids of varying surface tension [19]. The surface energy of the solid was defined to be equal to the surface tension of the liquid that wet the surface of the solid completely. This specific surface tension is defined as the critical surface tension.

Zisman's method requires multiple probe liquids and an accurate way to measure the contact angle of the liquid in question. Each liquid creates a unique contact angle with the surface. The definition of contact angle is the angle of the tangent of the drop curvature with the surface at the tri-phase point when the drop is viewed in profile and has come to equilibrium. Figure 1 illustrates the tangential line and the contact angle generated θ with the solid (*1*), liquid (*2*) and gas (*3*) phases.
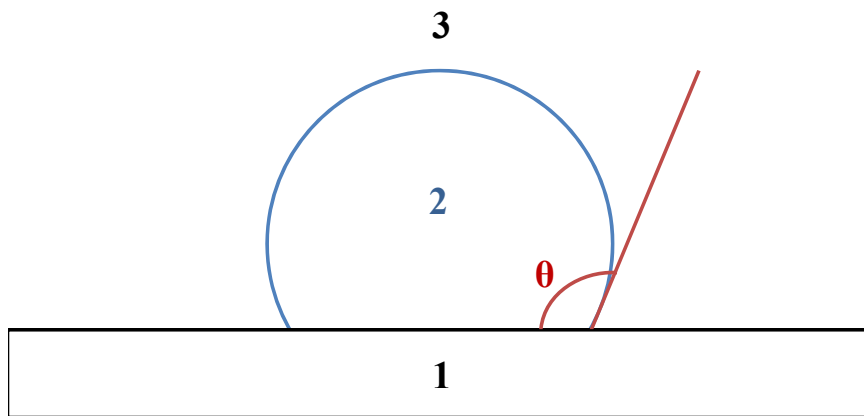
Figure 1. Contact Angle Definition

By measuring the contact angle of each liquid and then plotting the cosine of that angle against the surface tension, a linear relationship can be extrapolated to the point where the cosine of the contact angle equals one. The plot of this relationship is called the Zisman plot. The Zisman plot and theory can be applied to the concept of energy minimization in industry by using surface coatings as the probe liquids [19]. The best surface coatings must create the lowest surface energy and wet the entire surface completely. A Zisman plot can therefore be generated to compare a variety of coatings on the surface in question. Figure 2 is an example of the Zisman Plot:
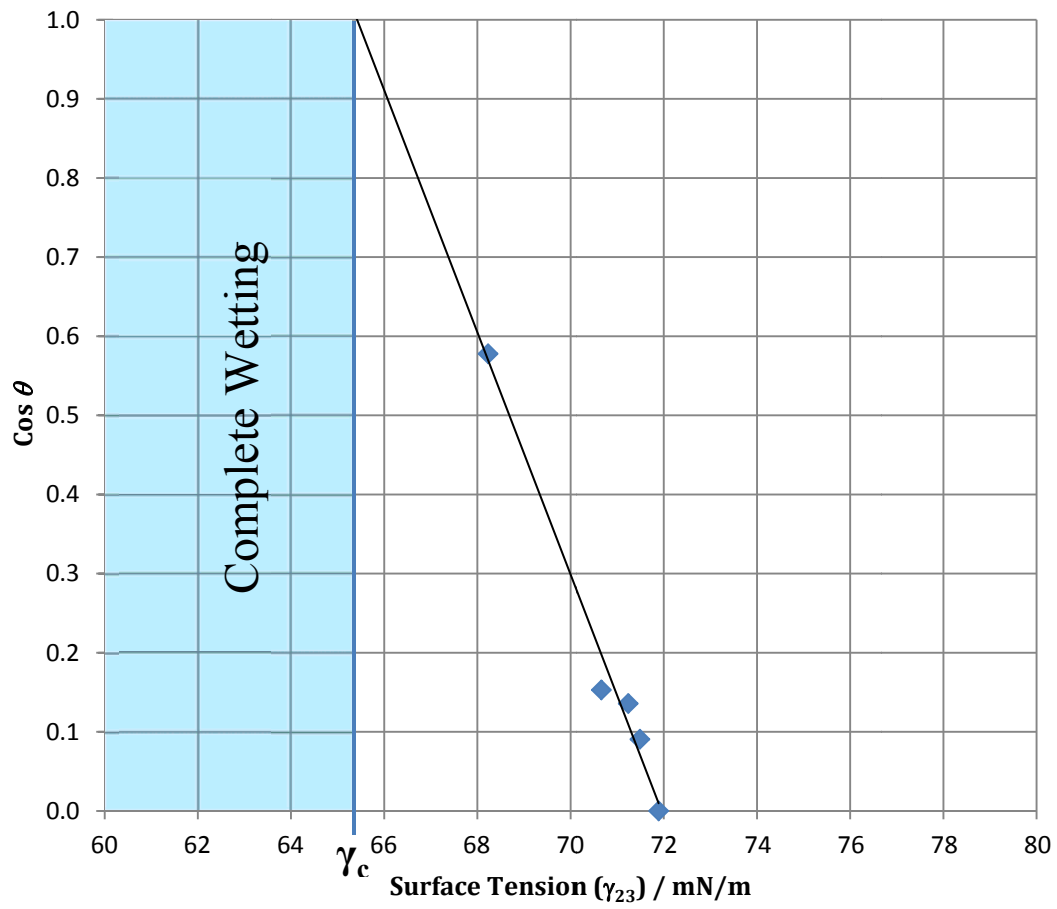
Figure 2. Example Zisman Plot

In the plot, the cosine of the contact angle is plotted versus the surface tension of

the liquid, γ. A linear line can be fitted to the surface tension measurements. A line is

then drawn from where cosine of the contact angle is equal to one across to intersect that

best fit line. At the intersection of the two lines lies the critical surface tension, γ_c, where

any liquid with a surface tension less than that will completely wet the surface in

question. The Zisman plot method is only valid for when the contact angle can clearly be

seen and the surface tension of every test liquid is known.

Du Nouy Ring Tensiometer

If one must determine the surface tension for a probe liquid, a du Nouy ring

tensiometer can be used. The tensiometer uses a platinum-iridium ring suspended just

below the surface level of the liquid. [20][21][22][23] The liquid adheres to the ring causing a

cylinder of liquid to be lifted above the surface, as seen in Figure 3. The mass of the

liquid lifted is proportional to the surface tension. The mass is measured by a digital scale

attached to a computer which provides a digital output similar to Figure 4.
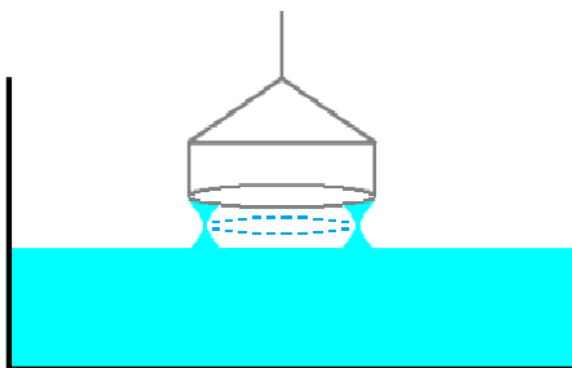
Figure 3. Ring Tensiometer Example

The force curve data in Figure 4 compares a solution of soapy water with a

concentration of 159 parts per million dish soap by mass to deionized (DI) water. The

curves effectively illustrate that by adding a surfactant to a solution, the force curve

changes with respect to the maximum force on the ring. The y axis illustrates the mass of

liquid on the ring while the x axis shows the time in seconds. The units of x and y can be

multiplied by the distance the ring was pulled to give the newtons of force for the liquid,

which is a measure of surface tension.
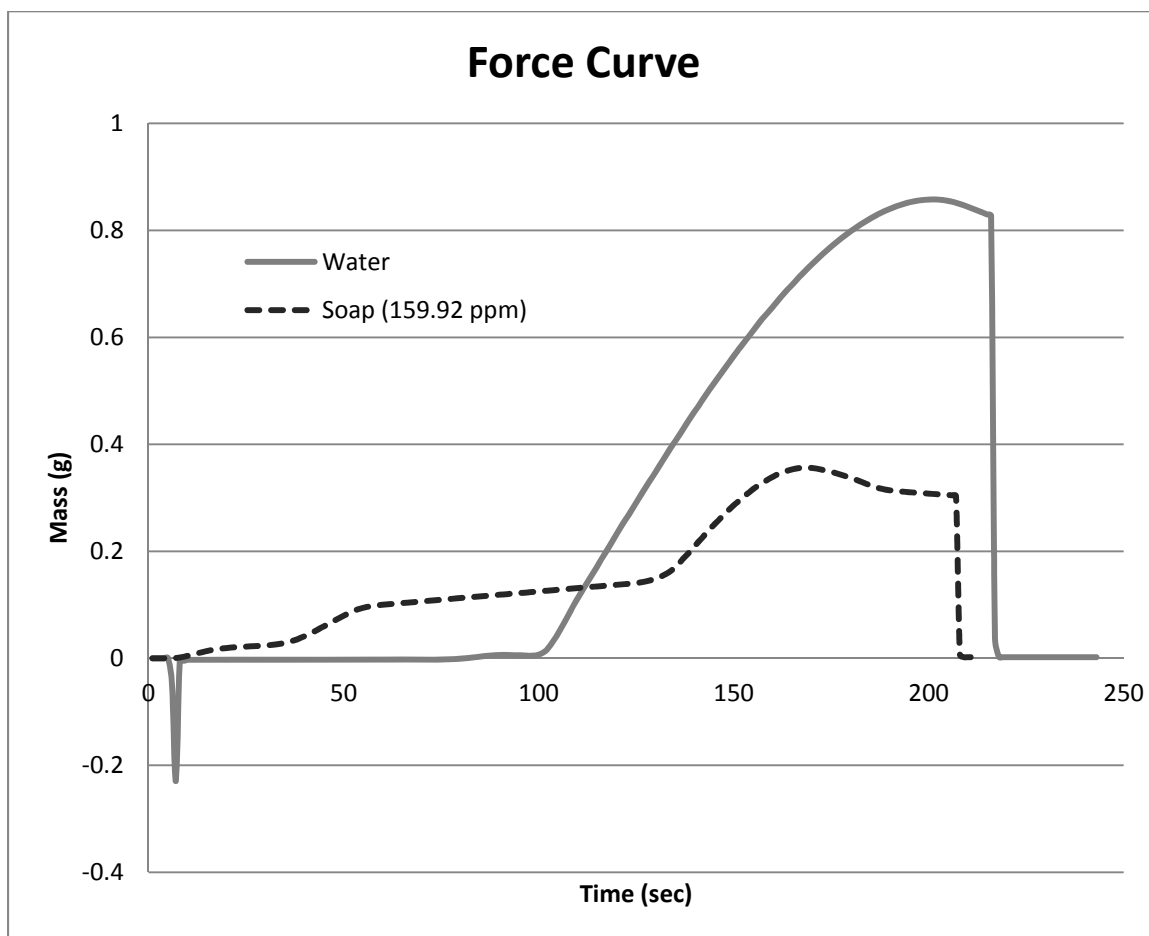
Figure 4. Ring Tensiometer Data Output Example

The ring tensiometer is well-accepted as a method to determine surface properties of a liquid. The tensiometer cannot determine any properties of a surface. To measure the properties of a surface, the sessile drop technique may be used, just as Zisman did.

Sessile Drop Technique

The surface properties of a solid surface can be studied using the sessile drop technique. The sessile drop technique requires a known volume of liquid to be placed on a surface using a pipette in the range of 1 to 20 microliters. The characteristics of the drop formed describe the relationship of the surface and the liquid in question. The analysis of

the contact angle of the droplet with the surface can then be used to characterize the surface energy of the surface.

The half-angle method for measuring the contact angle of a drop, θ, on a surface is defined using the base, *b,* and the height of the drop, *h,* as seen in Figure 5 and Equation 2:

$$\theta = 2tan^{-1}\left(\frac{2h}{b}\right) \tag{2}$$
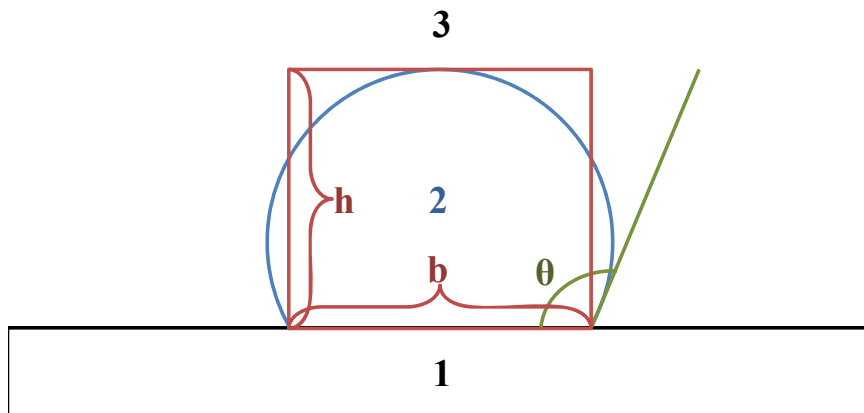
Figure 5. Half-Angle Method

The half-angle method is only appropriate for perfect spheres, but since not all drops are perfect spheres, other theories must be explored to account for imperfections in drops. The half-angle method focuses on the base length and the height of the drop. Other theories, including the Young equation, focus on the forces generated along the solid-liquid-gas interface.

The Young equation (Eq. 3) describes the contact angle, θ, between the surface (*1*), the liquid (*2*) and the surroundings (*3*) using the forces generated between each (γ) as measured in joules per meter [1]:

$$\gamma_{12} = \gamma_{13} + \gamma_{23}cos\theta \tag{3}$$

(a)

(b)
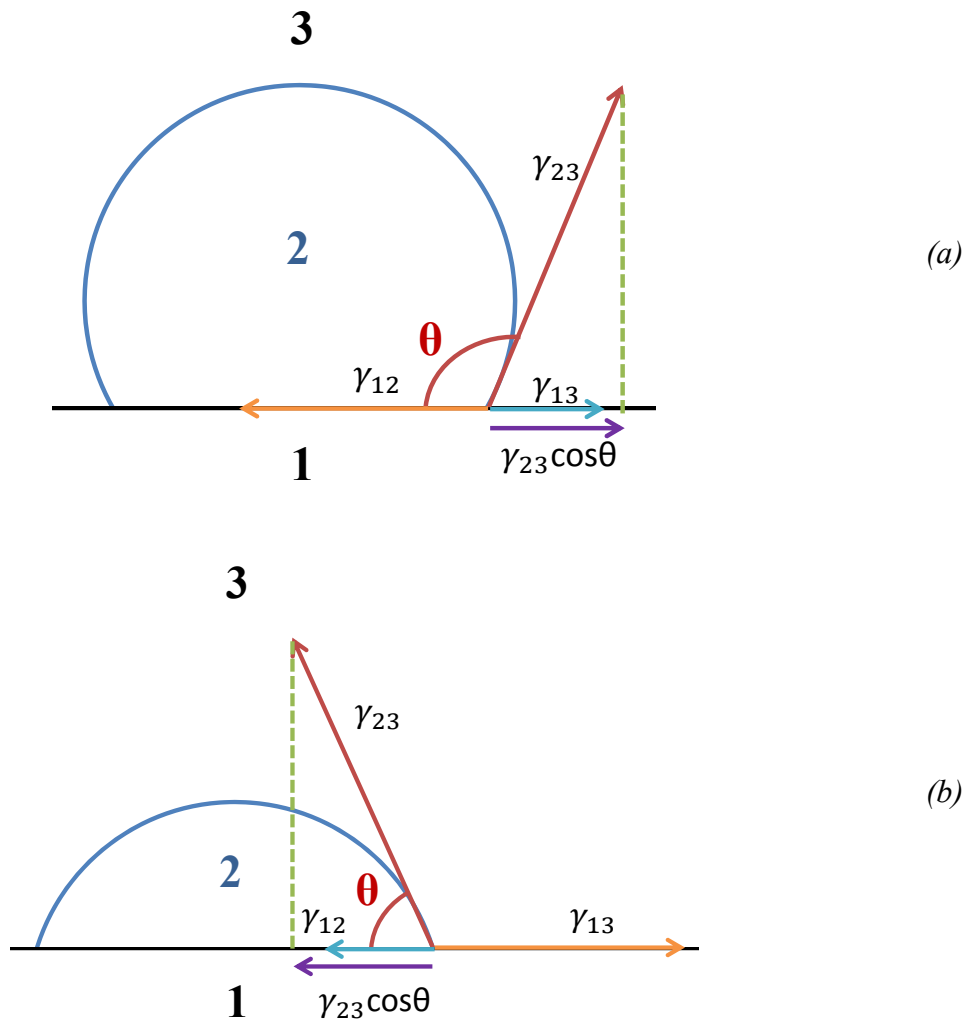
Figure 6. Sessile Drop on a Surface: (a) Greater than 90°, (b) Less than 90°

Figure 6 depicts a sessile droplet of liquid on a surface, with *(a)* showing a drop with a contact angle greater 90 degrees and *(b)* showing a contact angle of less than 90 degrees. By measuring the contact angle, θ, generated by the sessile drop, the tri-phase point, also known as the solid-liquid-air interaction point, can be analyzed. The contact angle is related to the amount of surface energy present. A low contact angle indicates a high surface energy of the solid and strong solid-liquid interactions. In such cases the

liquid spreads extensively to generate the lowest overall surface energy of the system. A high contact angle value indicates a low surface energy of the solid with less solid-liquid interaction. By working towards a point at which the total surface energy of the surface is minimized, the equilibrium or minimum energy is achieved.

The Young equation takes into account adhesive and cohesive forces while the Zisman method treats the surface energy as a single parameter. The single parameter approach, while simplistic, can be very precise so long as the surface energies of the probe liquids are well known. The sessile drop technique has been criticized because the contact angle results are often method and operator dependent. [24][25][26] Therefore, for the Zisman analysis to be successfully implemented, one must be able to refine the measurement techniques and operator skills. Method refinement and operator training is much more successful if one has a stable reference material or standard sample. Actual water drops are not suitable because the contact angle changes over time with vibration, evaporation, and contamination.

The direct use of the Young equation (Eq. 3) requires viewing the droplet from the side, but not all drops can be viewed from the side. By exploring the different ways a drop can be viewed, an improvement in the Young and Zisman approach to viewing the drop from the side might be made.

CHAPTER III

METHODS OF CONTACT ANGLE MEASUREMENT

There were three primary approaches to measuring solid substrates that mimicked drops; the side-on (Young [1]), top-down (Bikerman [15]) and reflected angle (Langmuir [13-14]) methods. The three methods have their own challenges and advantages when measuring a drop. One primary issue with all three is that the liquid drop is susceptible to the environment during measurement. When using solvents like hexane, the evaporation rate is much greater than solvents like water. In order to combat the problem of a drop changing shape during measurement through things like evaporation, a photograph of the drop is typically analyzed.

In using images for data analysis, it is important to first determine the picture quality and lighting so that there is an appropriate amount of contrast and clarity. A microscope is selected as the primary image collected as it is the most commonly used in current contact angle methods. The maximum resolution allowed by the DinoLite microscope of 1280 by 1024 pixels is used which allowed the user to zoom in a large amount without losing much of the drop's character. To help distinguish between the background and the drop, all of the images are converted to black and white allowing the droplet's edge to be crisper and easier for the drop shape analysis techniques to measure. The addition of a secondary light source and diffuser beyond the room lighting also helps provide better contrast between the standard and background. The diffuser is a piece of polystyrene cut to fit just around the secondary light source.

Since the picture allowed for the drop to be frozen in time, any number of researchers can analyze the drop image at any point in time.Multiple attempts at analyzing the images allows the estimation of variability between analysts to be assessed when measuring the contact angle. Only the reflected angle method, specifically the Contact-θ-Meter [13], uses its own apparatus for measurement so no pictures are necessary. The data from all of the methods explored were compared and statistically analyzed for precision and accuracy in MiniTab [27].

Side-On Methods

The first method mimics both Young and Zisman's approach to contact angle measurement. By viewing the drop from the side, the two tri-phase points on either side of the drop are easily visible. The best view of the tri-phase point places a camera perpendicular to the side of the drop. Figure 7 is a schematic of a side-on method using a digital microscope:
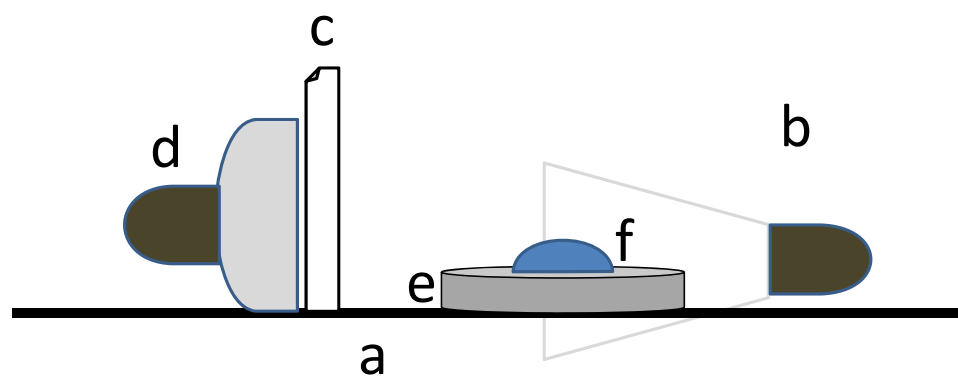
Figure 7. Apparatus for Side-On Contact Angle Measurement

In Figure 7, *a* is the stage, *b* is the camera, *c* is a diffuser, *d* is the incandescent light source, *e* is the surface in question, and *f* is the droplet.

The first apparatus, although effective, is limited as far as portability and has a hard time measuring contact angles above the plane of the surface which is essential for measuring the contact angle of a droplet on a large surface. Since one goal of this research is to create a more usable apparatus in the field, two other methods were developed; one using a mirror and another using a prism to reflect the view of the side of the drop to the camera. Several types of mirrors were investigated, including highly polished stainless steel and a back silvered mirror. Figure 8 is a schematic of the mirror and prism using the digital microscope:
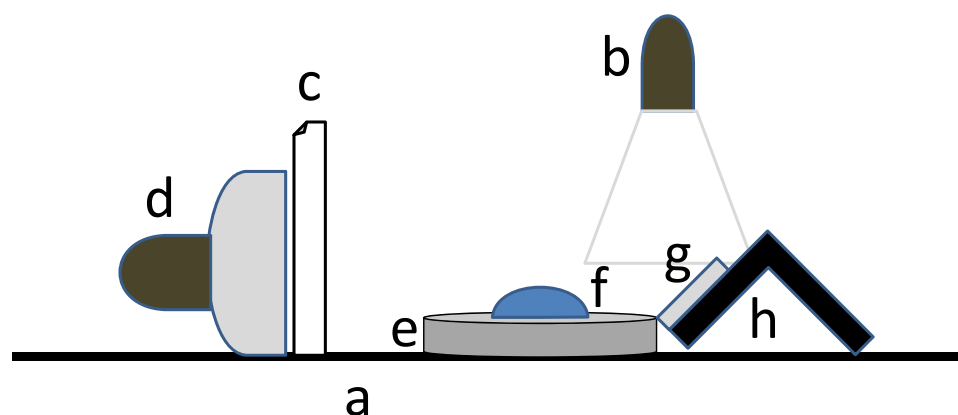
Figure 8. Apparatus for Mirror and Prism Methods

In Figure 8, *a* is the stage, *b* is the camera, *c* is a diffuser, the incandescent light source is *d, e* is the sample with the sessile droplet *f*, and *g* and *h* are the polished silver mirror and aluminum mount, respectfully. The mirror and holder, *g* and *h*, can be replaced by a prism, or by a one-piece polished steel coupon bent by 90 degrees.

The mirror and prism reflect an image of the drop from the side into the camera positioned above the drop. The mirror or prism allows for the camera to be placed on a surface of any size while also providing a clear view of the tri-phase point. It is therefore

necessary to have the reflection of the drop on the surface visible in the image. The reflection of the drop is critical to view the tri-phase point. The tri-phase point is needed when using the drop shape analysis software to analyze the drops for their contact angles, specifically the half-angle, and Brugnara methods. [24, 28]

The Brugnara method uses the ImageJ [29] program combined with the Contact Angle plugin [28]. The plugin requires the user to define five points along the edge of the drop. A circle or ellipse is then fit to these points by the software in manual mode. A second option was the Both Best Fits approach which uses a first derivative filter to determine the edge of the drop (Canny-Deriche Filtering [30].)

In order for the first derivative to be the most accurate value, the minimum and maximum threshold values must be manipulated so that the thinnest line of points along the edge of the drop is obtained. After the threshold is optimized visually by the analyst, the resultant output file displays the contact angle of the circle, and the left, right, and average contact angles of the ellipse. The data output from the plugin can be replicated by any number of users since it uses a picture rather than a live sample.

Top-Down Methods

J. J. Bikerman postulated the idea of using small sessile drops on surfaces to measure the surface tension of the liquid. He understood that a large droplet would be influenced by gravity; therefore Bikerman chose to use small droplets that he could be confident were spherical. He would place a droplet on a surface, and then sprinkle talc over it. The surfactant was then allowed to evaporate, leaving a ring of powder equaling the base contact diameter of the drop. [15]

Since the drop was defined as spherical, Bikerman derived the influence of the ratio of the drop's base contact diameter, b, and its volume, v, to the angle the drop forms with the surface, θ, in the following equation:

$$\frac{b^3}{v} = \frac{24\sin^3\theta}{\pi\,(2 - 3\cos\theta + \cos^3\theta)} \tag{4}$$
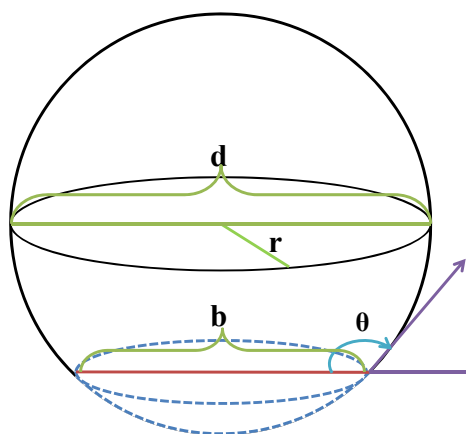
Figure 9. Equation 4 Explanation

The equation requires that the drop be spherical, and this restricts the volume of the drops to within the microliter range.

The powdered surface may be used so long as the ring it forms around the edge of the drop is left in exactly the same place once the actual surfactant has evaporated. Since not all surfactants evaporate equally across every drop, it is possible to develop a receding contact angle as the drop is evaporating which can lead to a decisively smaller diameter and therefore skewed diameter and contact angle measurements.

In the original experiment, Bikerman used a microscope fitted with a micrometer eyepiece to measure his drop diameters, but suggests that any measurement method may be used. Variability by one percent in measuring base contact diameters of drops will increase the uncertainty in the ratio to three percent necessitating the need for a more

precise way of measuring the drop's base contact diameter. Therefore the picture method allows for an immediate measurement of the drop's base contact diameter.

The top-down method mimics the way Bikerman measured the contact angles except that the microscope is replaced with an apparatus similar to the mirror and prism methods except the mirror or prism is removed. Figure 10 is a schematic of that apparatus where *a* is the stage, *b* is the camera, *c* is diffuser, and the incandescent light is *d*. The surface, *e,* then has droplet *f,* which is the drop of solvent being investigated and the calibration object *g*.
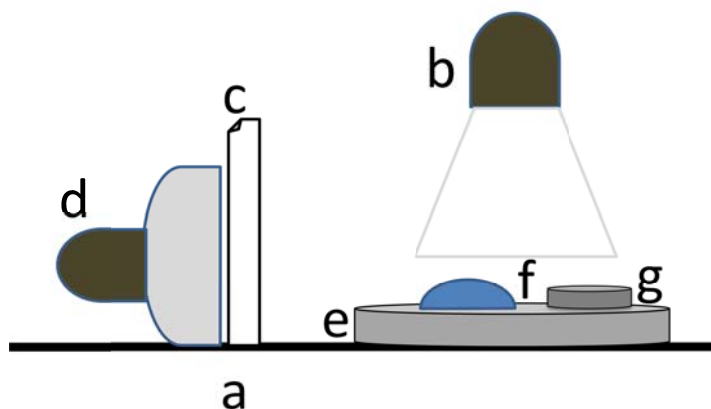
Figure 10. Schematic for Top-Down Method

As with the improvements made to the side-on method, the top-down method can be improved in portability and marketing by using cell phone cameras rather than a microscope. Williams, *et al.* [25], suggests that cell phone macrophotography using auxiliary lenses can improve image quality enough for drop shape analysis thus eliminating the need for the digital microscope and computer set up. The iPod has a macro lens attached to it to provide better image quality and a stand to hold it steady at 90 degrees elevation or perfectly perpendicular to the drop as seen in Figure 11. The apparatus is shown upside down to illustrate the lens and the stand may be seen.
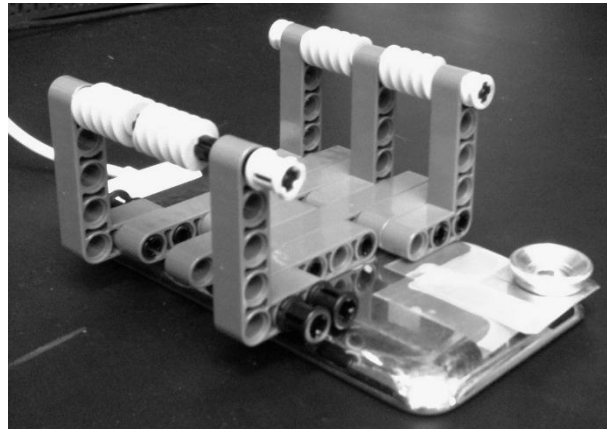
Figure 11. Top-Down iPod Device

     The Williams paper also suggests that when measuring drop diameters, a calibration object is necessary for decreasing error, and improving precision and accuracy. By using the Meazure [31] program to measure the diameter of the drop as well as the calibration object, a conversion from image pixels to millimeters can be made.

     By using Meazure or ImageJ, any imperfections in the drop's diameter can be observed. If the drop is oblong in shape, the long and short diameters will be measured and averaged to provide the average diameter. The diameter can then be plugged into Equation 4, so long as the volume is known, and can then provide the average θ.

     Should the drop's contact angle be greater than 90 degrees, Equation 4 is useless. In order to measure contact angles of greater than 90 degrees, a second equation must be used. Equation 5, as derived in Appendix C, mathematically explains the change.

$$\frac{d^3}{v} = \frac{24}{\pi\,(2 - 3cos\theta + cos^3\theta)} \tag{5}$$

     Equations 4 and 5 can be combined to form a Top-Down Calculator spreadsheet, as explained by Williams, *et al.* [25] In the paper, Williams constructs a spreadsheet which uses known contact angles to calculate the contact diameter/ volume ratio. Then, a second

chart generates a plot of the Bikerman equation using the drop's base (*b*) contact diameter (Eq. 4) and the equation using the diameter (*d*) of the drop (Eq. 5). The calculator then uses the VLOOKUP function and volume of the drop in question to find the contact angle of the drop depending on the measured diameter.

The volume of the drop is measured independently, but the spreadsheet does make it possible for the fast analysis of drops simply by measuring the diameter. The Top-Down Calculator spreadsheet combined with the top-down method decreases the size of the apparatus in question and allows for the repeatability of measurements of the drop's diameter as any number of users can measure the picture and then compare their results rapidly and effectively.

Reflected Angle Methods

The final method investigated here is the reflected angle method. In measuring contact angles of sessile drops it is important to note the Contact-θ-Meter, which is based upon a method described by Irving Langmuir in 1937 [32]. The Contact-θ-Meter uses a small beam of light to illuminate a drop from the side. The user looks through a viewing tube, *d*, at the edge of the drop. The tube is moved around a pivot until the illumination source as seen near the tri-phase point disappears. The angle of the pivoting viewing tube is calibrated to display contact angle on the LCD display, *b*. All of the electronics are housed in *a*. An image of the device is seen in Figure 12.
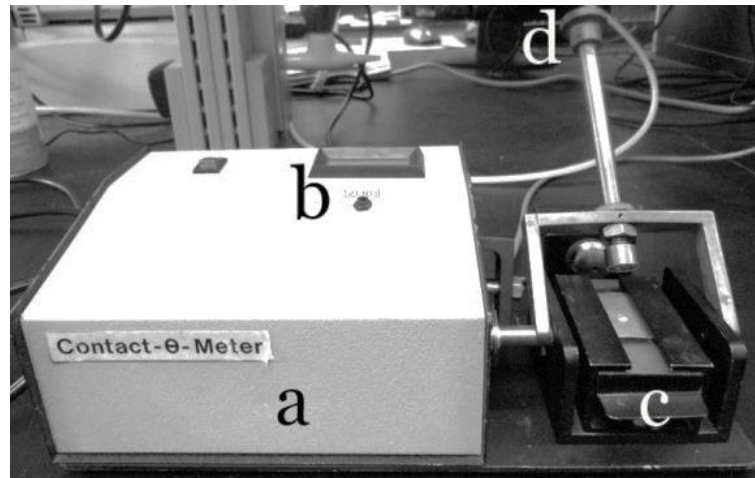
Figure 12. Contact-θ-Meter

The Contact-θ-Meter requires the droplet of liquid be placed on a removable

stage, *c*. The stage limits the user to small surfaces that can be cut down to fit on the stage

and the drop must have a contact angle of less than 90 degrees as the light cannot be

reflected properly off angles greater than that. Figure 13 illustrates how the light hits the

droplet from the Contact-θ-Meter, where *i* is the incident ray of light, *R* is the reflected

ray of light, n_d is normal to the drop, and *T* is the tangent to the drop. The right side of the

image mimics a contact angle of less than 45 degrees while the left side mimics a contact

angle close to 90 degrees. Equation 6 calculates the contact angle.

$$\theta = 90° - \frac{\varphi}{2}$$
(6)
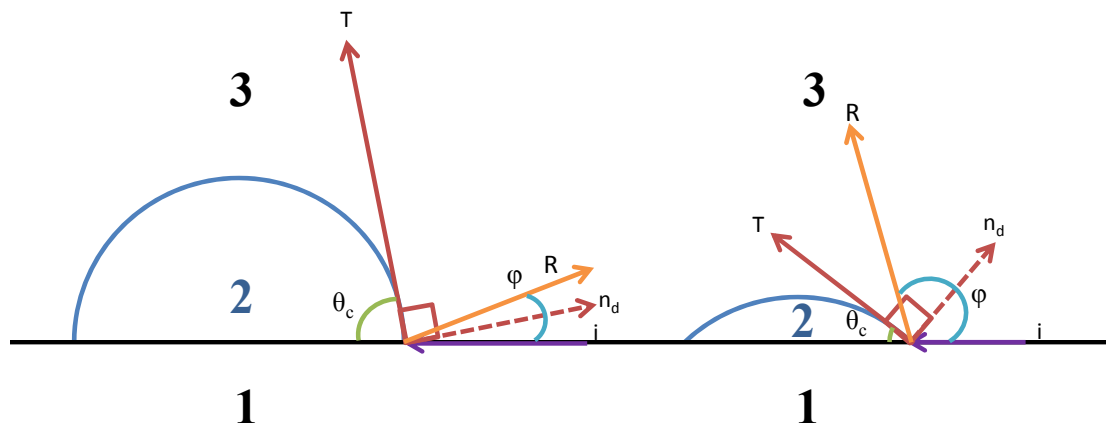
Figure 13. Light Reflected Off a Drop in Langmuir Method

When the contact angle is above 90 degrees, the light is reflected off of the drop into the solid. A contact angle less than 90 degrees allows for the light to reflect up off the droplet into the viewing tube so that the contact angle can be measured. The small stage size limitation and angle requirement are removed when using the modified iPod or cell phone cameras.

In order to mimic the Contact-θ-Meter, a small fiber-optic light was used to illuminate the drop. Then an iPod application called Theodolite[33] was used to take an image. Theodolite measures the elevation angle of the optical center line of the iPod camera. The application was used to mimic the Contact-θ-Meter and the elevation angle was used to determine φ and θ in Equation 6. Figure 14 shows an image of the iPod device when mimicking the reflected angle method.
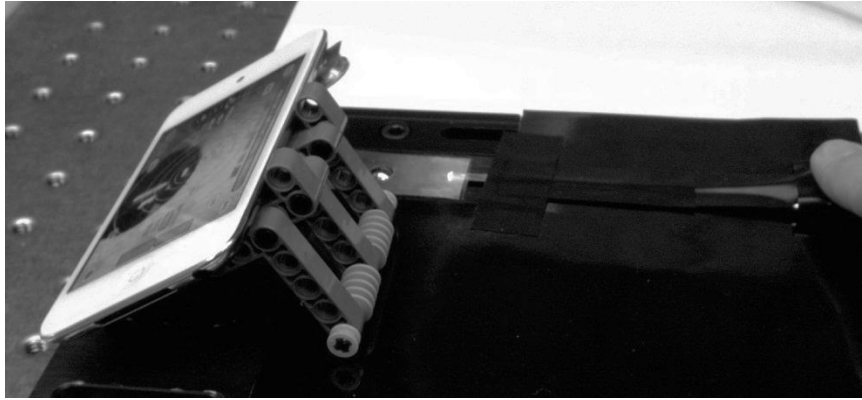
Figure 14. Reflected Angle iPod Device

The side-on, top-down and reflected angle methods will all be analyzed for precision, accuracy, and ease of use in the field. The side-on method will help analyze the half-angle method and the Young approach while the top-down method of Bikerman and the reflected angle method using the Contact-θ-Meter will also be analyzed. The preferred method is one that is accurate, precise, compact and portable/easy to use for the manufacturing technician and useful for large surfaces.

CHAPTER IV

PROPOSED TYPES OF STANDARDS

The side-on, top-down and reflected angle methods all have unknown precision and accuracy. Analyzing pictures alleviates some of the uncertainty as the drops are frozen in time so they remain unaffected by environment, but further uncertainty remains in the different methods. There are different steps associated with each method and each step contributes differently to the total uncertainty.

In order to lessen this uncertainty as well as to be able to compare methods, a standard has been developed. By creating a standard that can be measured by all three methods, the uncertainty in measuring variable liquid drops is eliminated. A standard also allows for the ability to compare different methods so any new approach could be accurately assessed.

Ball in a Hole

The first type of standard uses a spherical ruby ball with a 6 mm diameter (Edmund Optics #NT43-830) designed for use in a ball bearing, mounted in a drill gage card (Grainger #5C732) hole. The ruby ball acts as a non-evaporating standard which simulates a sessile drop without being affected by environmental changes. The accuracy and precision in the machining of the gage card holes and the ruby ball allows the use of it as a standard for the side-on contact angle measurement method. The gage card is used to ensure the size of drill bits and the holes the bits drill meaning that the gage card must be precise. The ruby ball is designed for use in a ball bearing so any irregularities in the shape or surface would prevent the bearing from working properly. Therefore the

machined nature of both the gage card and ruby ball lend themselves to creating a standard by placing the ruby ball into different holes on top of the gage card to mimic a series of contact angles greater than 90 degrees.

A less expensive steel ball with a quarter of an inch diameter (MSC Industrial Supply Co. #00072702) designed for use in a ball bearing was also evaluated. These highly spherical balls satisfy the requirements of spherical drops in using the half-angle, Bikerman, and Brugnara methods. Balls used in bearings are highly spherical as any imperfection in the ball would cause friction and therefore decrease their ability to perform their intended function. The steel ball provides a less expensive alternative to the ruby ball.

Pressed Aluminum Foil

A pressed aluminum foil standard is another attempt to make an inexpensive alternative to the ruby ball. A solid, non-evaporating aluminum standard is generated from pressing aluminum foil in a drill gage card hole to form a circular drop shape. The hole has the same diameter as the ruby ball thereby allowing them to be comparable.

In summary, the ruby ball and steel ball will be used to create standards of both greater than and less than 90 degrees, while the pressed aluminum foil can only mimic a drop with a contact angle of less than 90 degrees. Each standard will be measured using the side-on method and reflected angle method, but the standards of less than 90 degrees will also be measured using the top-down method. Once measured, a "lab accepted value" for their contact angles will be determined and then used to compare the accuracy of the methods and devices.

CHAPTER V

RESULTS

In order to compare the methods, an accepted value for the contact angle of each of the standards needed to be defined. The aluminum foil (*Al Foil*) and the under-mounted steel ball (*U-Steel*) mimic drops with contact angles of less than 90 degrees while the ruby ball (*Ruby*) and the steel ball (*Steel*) mimic drops with the contact angles of greater than 90 degrees. Each standard must have its own accepted value. The images taken of the standards using the side-on approach with the digital microscope (*Dino-S*) and then analyzed with the Manual Points Procedure provided the lab standard method because this approach most closely matches the current lab practices in industry.

Table 1, Table of the Accepted Values

Standard	Mean $\bar{x}$ (°)	Standard Deviation s (°)	N
1. Al Foil	$33._5$	0.5_0	5
2. U-Steel	$46._3$	0.3_0	5
3. Ruby	$115._2$	0.5_0	5
4. Steel	$117._9$	0.6_8	5

Once an accepted contact angle was defined for each of the standards, the error between the digital microscope without the mirror (*Dino-S*), the digital microscope with the mirror (*Dino-M*), and the iPod with the mirror (*iPod-M*) could be calculated.

Table 2, Table of Contact Angle Measurements Using Side-On Methods

	Dino-S		Dino-M		iPod-M		
Standard	$\bar{x}$ (°)	s (°)	$\bar{x}$ (°)	s (°)	$\bar{x}$ (°)	s (°)	N
1. Al Foil	$32._7$	2.1_7	$31._8$	0.5_2	$31._3$	2.4_5	15
2. U-Steel	$46._3$	0.3_4	$44._2$	0.6_5	$40._5$	4.2_0	15
3. Ruby	$115._7$	0.8_8	$109._7$	1.1_3	$110._4$	0.5_8	10
4. Steel	$117._9$	0.4_8	$115._5$	1.1_6	$116._3$	1.2_7	10

The measured error calculations were done using all three methods of analysis, the Circle Best Fit (*C*) and Manual Points (*M*) procedures in Brugnara, and then the half-angle method (*H*). The *N* value corresponds to each method of measurement. For example, the ruby ball was measured ten times with the side-on approach using the microscope, ten times with the microscope/mirror, and ten times with the iPod/mirror set-up.

The half-angle method is done by using the ImageJ program's square selection tool. The square is aligned at the two tri-phase points to create the base and then stretched to the top of the standard to provide the height. The Manual Points Procedure requires the analyst to place a point on the tri-phase point on either side of the standard, and then three more points around the standard. Once the points are added to the image, the computer attempts to fit a circle and ellipse to those points. The plugin then provides the angles of the circle and the ellipse in a data output file. The circle value was chosen in each case as the standards are as close to circular as possible. The Circle Best Fit approach attempts to also fit a circle to the standard, but instead using threshold values. The threshold values

are set so that the points drawn on the image in red line up to the edge of the standard. The difference between the Manual Points and Circular Best Fit procedures is that the Manual procedure uses the user imputed values to calculate the contact angle while the Circular procedure uses the computer. As Williams, *et al.,* [24] showed, the Circle Best Fit is only appropriate for images with good contrast, while the Manual Points Procedure could use lesser quality images.

In order to account for the error in each of the three procedures, analysis in MiniTab was done to generate a boxplot of all the data partitioned by standard.
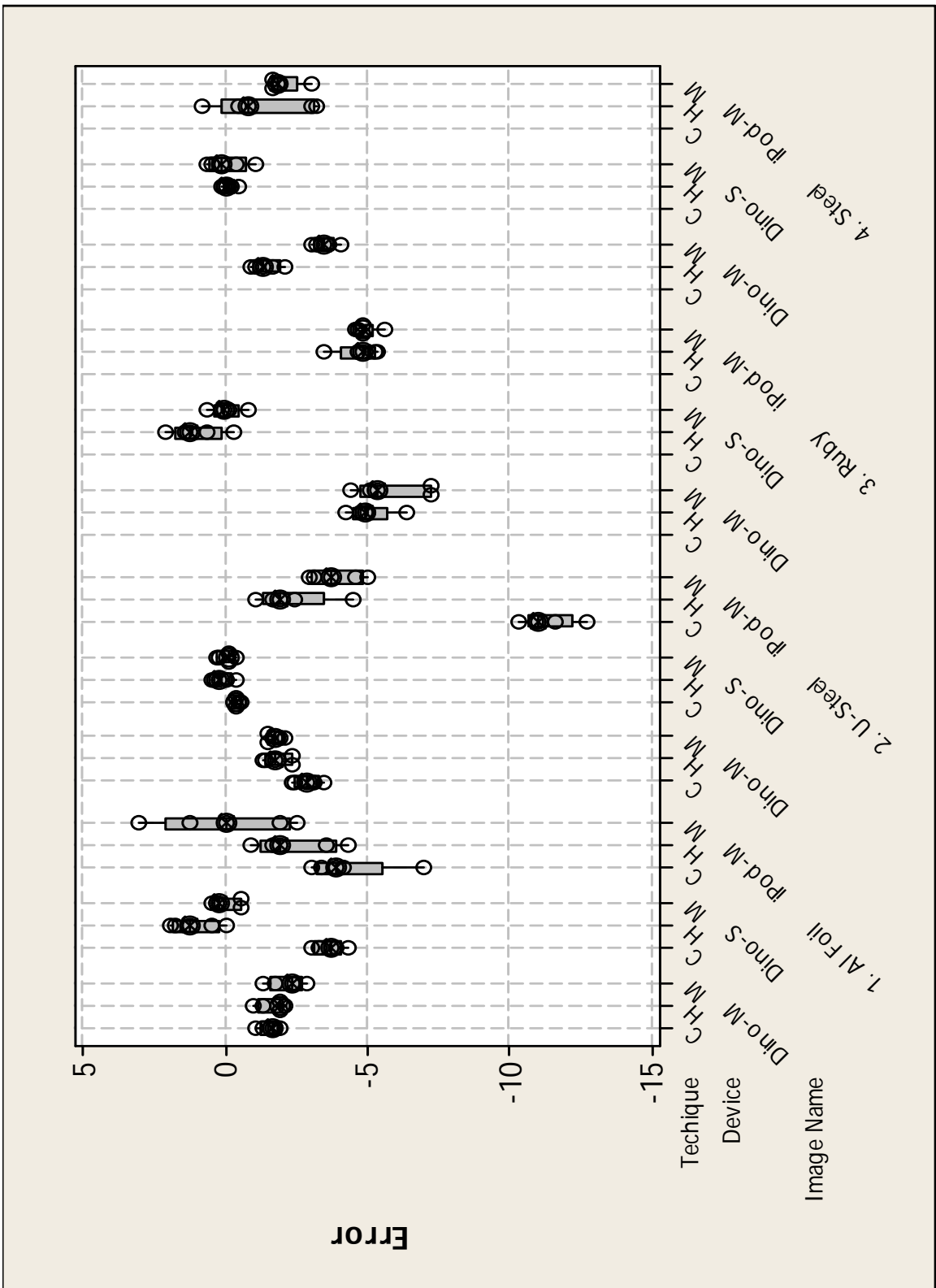
Figure 15. Boxplot of Error Partitioned by Standard, Device, and Technique

To clarify, Figure 15 was broken down into four separate boxplots, one for each of the types of standards in Figures 16 through 19.
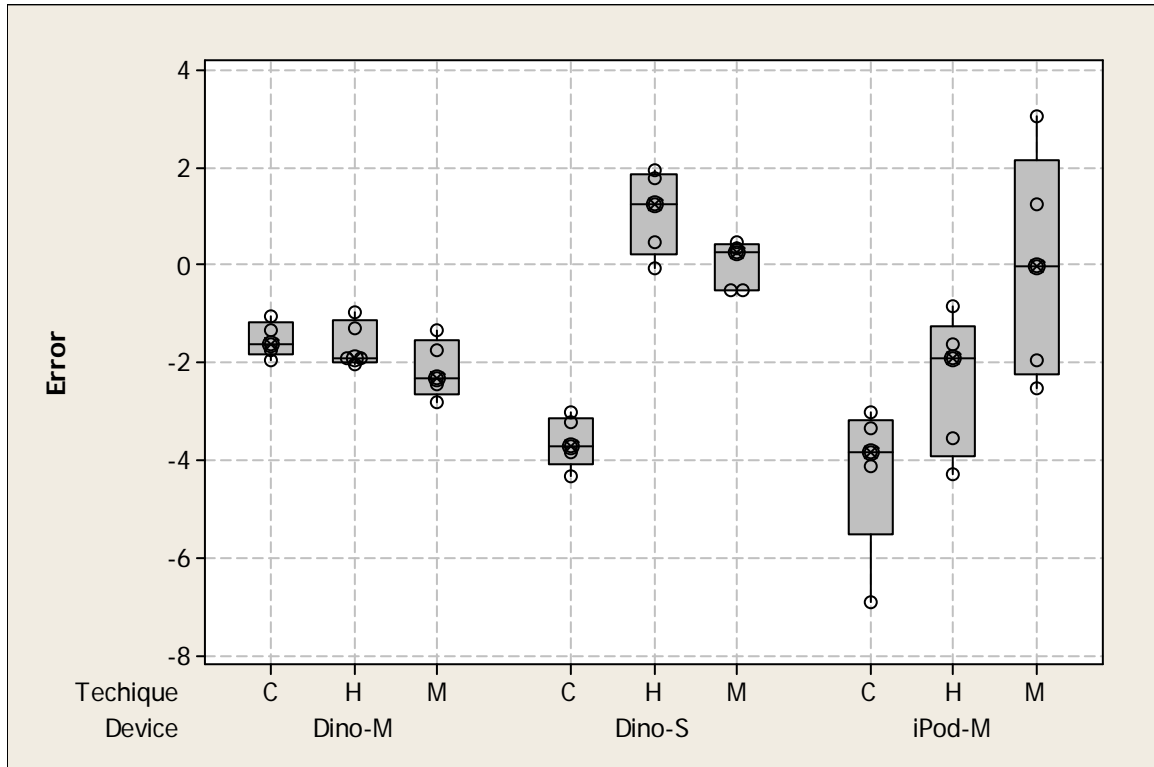
Figure 16. Boxplot of Error Partitioned by Device and Technique for the Aluminum Foil Standard

Table 3, Data of Error Partitioned by Device and Technique for the Aluminum Foil Standard

Device	Analysis Technique	$\bar{x}$ (°)	s (°)	N
Dino-M	C	$-1._5$	0.3_5	5
	H	$-1._6$	0.4_7	5
	M	$-2._1$	0.6_0	5
Dino-S	C	$-3._6$	0.5_1	5
	H	$1._1$	0.8_5	5
	M	$0._0$	0.5_0	5
iPod-M	C	$-4._3$	1.5_6	5
	H	$-2._5$	1.4_2	5
	M	$0._0$	2.3_0	5
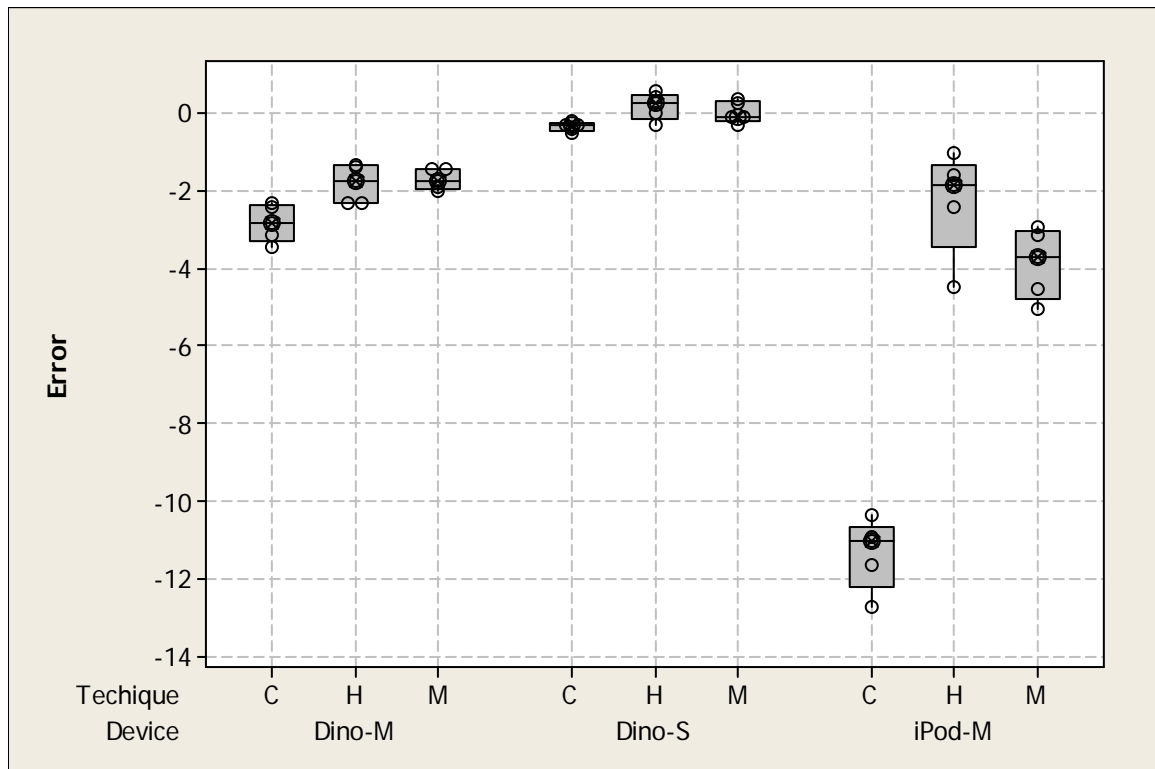
Figure 17. Boxplot of Error Partitioned by Device and Technique for the Under-mounted Steel

Ball Standard

Table 4, Data of Error Partitioned by Device and Technique for the Under-mounted Steel Ball

Standard

Device	Analysis Technique	$\bar{x}$ (°)	s (°)	N
Dino-M	C	$-2._8$	0.4_6	5
	H	$-1._8$	0.4_8	5
	M	$-1._7$	0.2_8	5
Dino-S	C	$-0._4$	0.1_1	5
	H	$0._2$	0.3_4	5
	M	$0._0$	0.3_0	5
iPod-M	C	$-11._3$	0.9_1	5
	H	$-2._3$	1.3_3	5
	M	$-3._9$	0.9_0	5
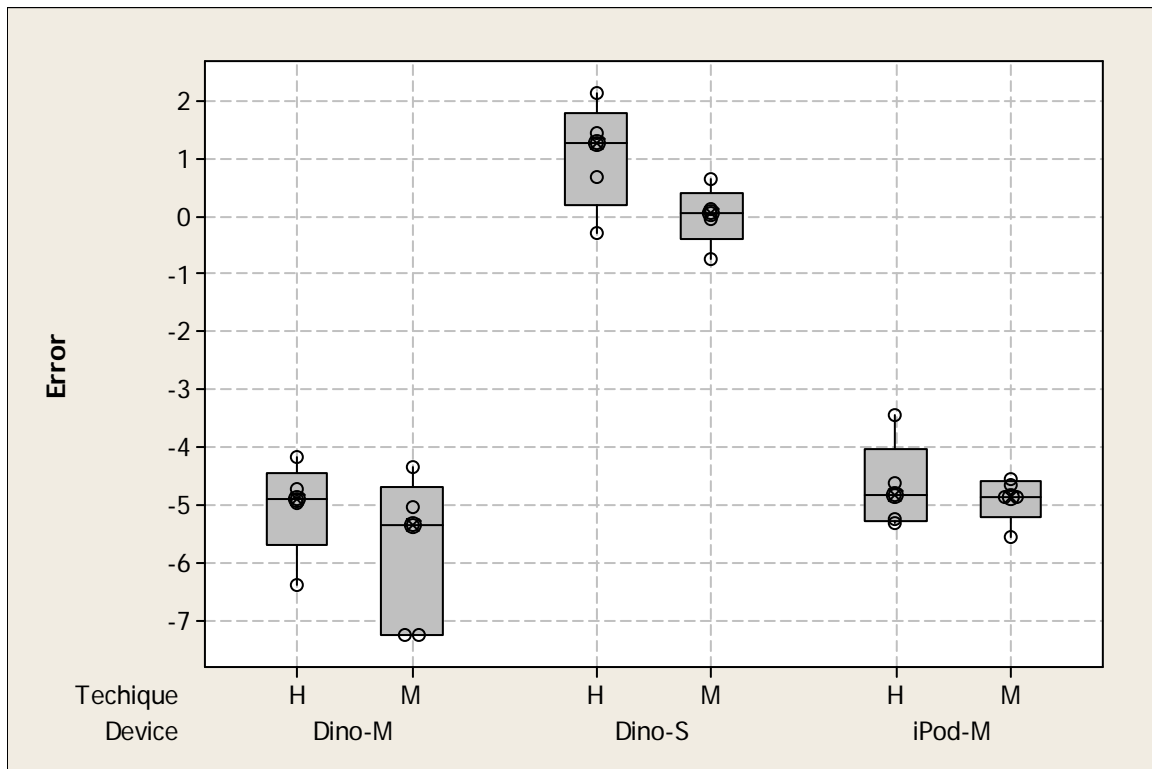
Figure 18. Boxplot of Error Partitioned by Device and Technique for the Ruby Ball Standard

Table 5, Data of Error Partitioned by Device and Technique for the Ruby Ball Standard

Device	Analysis Technique	$\bar{x}$ (°)	s (°)	N
Dino-M	H	$-5._0$	0.8_2	5
	M	$-5._9$	1.3_3	5
Dino-S	H	$1._1$	0.9_1	5
	M	$0._0$	0.5_0	5
iPod-M	H	$-4._7$	0.7_5	5
	M	$-4._9$	0.3_9	5
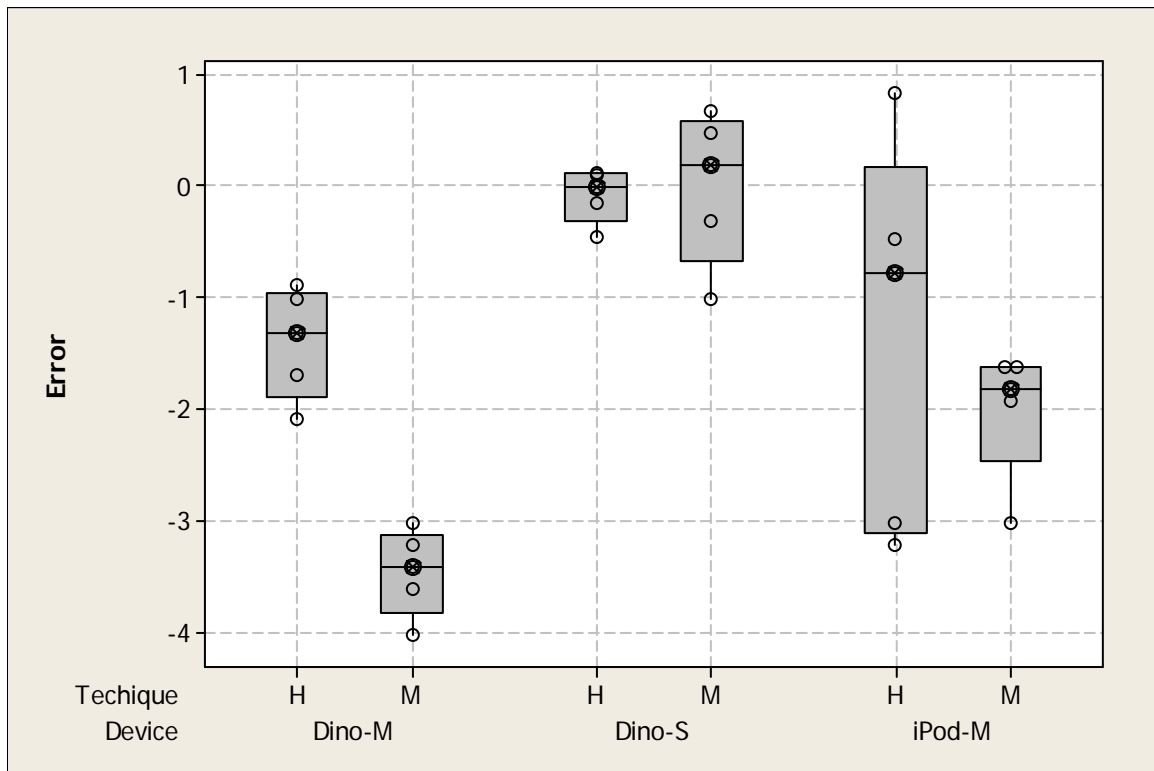
Figure 19. Boxplot of Error Partitioned by Device and Technique for the Steel Ball Standard

Table 6, Data of Error Partitioned by Device and Technique for the Steel Ball Standard

Device	Analysis Technique	$\bar{x}$ (°)	s (°)	N
Dino-M	H	$-1._4$	0.4_9	5
	M	$-3._5$	0.3_8	5
Dino-S	H	$-0._1$	0.2_4	5
	M	$0._0$	0.6_8	5
iPod-M	H	$-1._3$	1.7_4	5
	M	$-2._0$	0.5_8	5

In simplifying the boxplot in Figure 15, a secondary boxplot was created to evaluate the error in the contact angle for the standards based on whether or not a mirror was used by grouping the steel ball and ruby ball as the greater than 90 degree group and the under-mounted steel ball and the pressed aluminum foil as the less than 90 degree group..
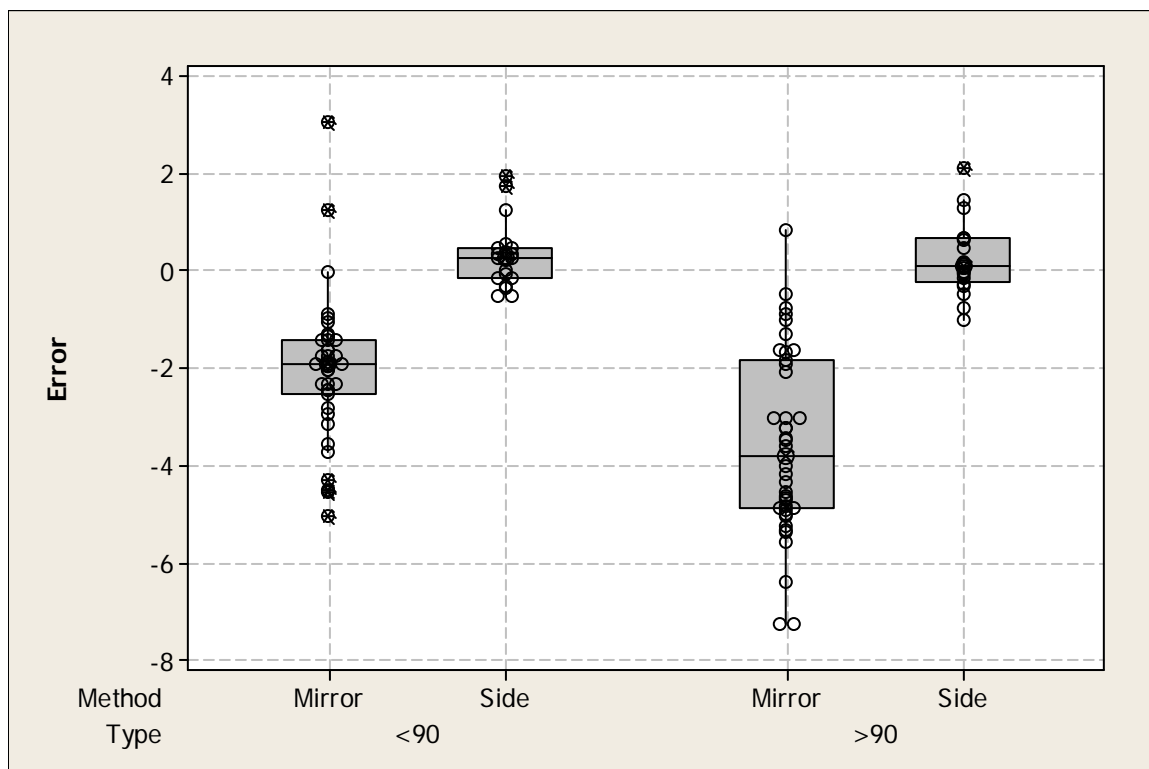
Figure 20. Boxplot of Error Based on the Presence of a Mirror

Table 7, Data of Error Based on the Presence of a Mirror

Device	Mirror/No Mirror	$\bar{x}$ (°)	s (°)	N
1. Al Foil	Mirror	$-1._6$	1.6_0	20
	Side	$0._5$	0.8_7	10
2. U-Steel	Mirror	$-2._4$	1.1_8	20
	Side	$0._1$	0.3_1	10
3. Ruby	Mirror	$-5._1$	0.9_3	20
	Side	$0._5$	0.8_8	10
4. Steel	Mirror	$-2._0$	1.2_5	20
	Side	$0._0$	0.4_8	10

A third analysis of the data evaluated the usefulness of a screen over the drop which reduced glare from the room lights. The screen was made from a rectangular cap built to be adjustable so that it could be placed on top of the standard to help reduce the reflection of the room light off the top of the standard.

The following boxplot graphically represents the error in the images, no matter the analysis method, based on the presence or absence of a screen.
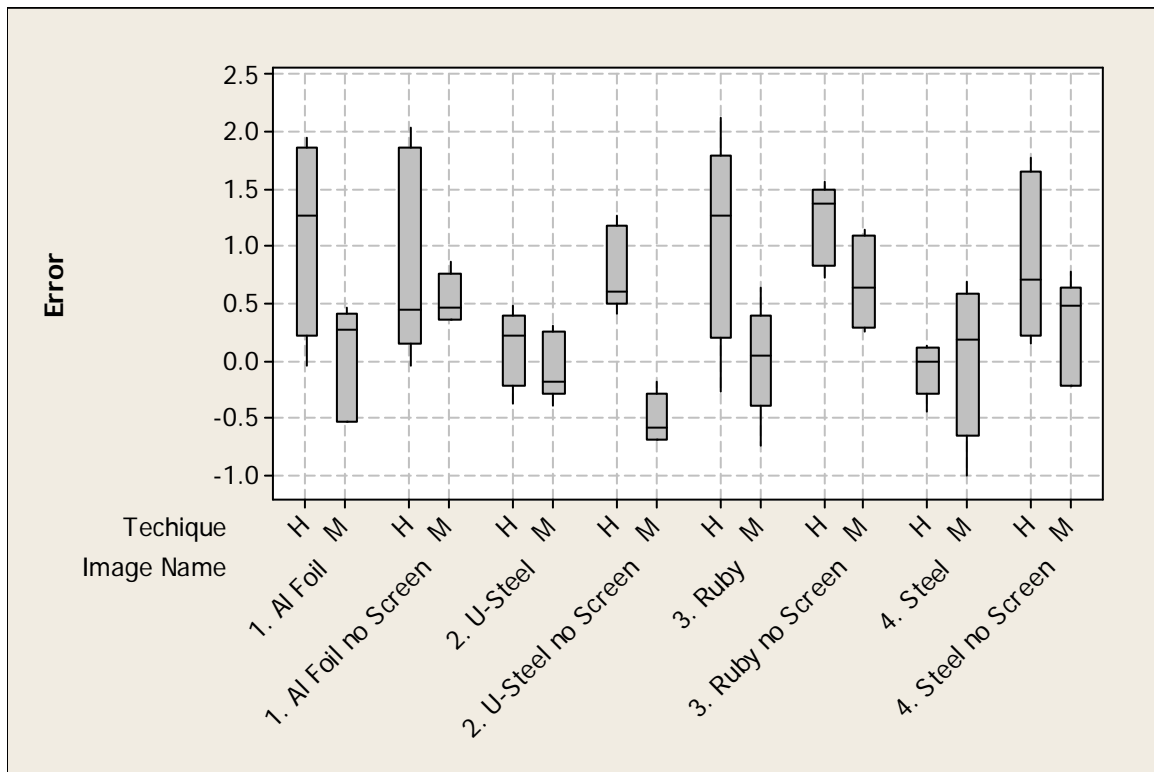
Figure 21. Boxplot of Error with Respect to the Presence or Absence of a Screen

Table 8, Data of Error Based on the Presence of a Screen

Device	Analysis Technique	$\bar{x}$ (°)	s (°)	N
1. Al Foil	H	$1._1$	0.8_5	5
	M	$0._0$	0.5_0	5
1. Al Foil no Screen	H	$0._9$	0.9_1	5
	M	$0._5$	0.2_2	5
2. U-Steel	H	$0._1$	0.3_4	5
	M	$-0._1$	0.3_0	5
2. U-Steel no Screen	H	$0._8$	0.3_7	5
	M	$-0._5$	0.2_2	5
3. Ruby	H	$1._1$	0.9_1	5
	M	$0._0$	0.5_0	5
3. Ruby no Screen	H	$1._2$	0.3_6	5
	M	$0._7$	0.4_0	5
4. Steel	H	$-0._1$	0.2_4	5
	M	$0._0$	0.6_8	5
4. Steel no Screen	H	$0._9$	0.7_4	5
	M	$0._3$	0.4_5	5

The top-down Bikerman method was restricted to the two standards that exhibited contact angles of less than 90 degrees, the aluminum standard and the under-mounted steel ball. Figure 22 shows the boxplot of error depending on the standard as well as on the device used to analyze the image.
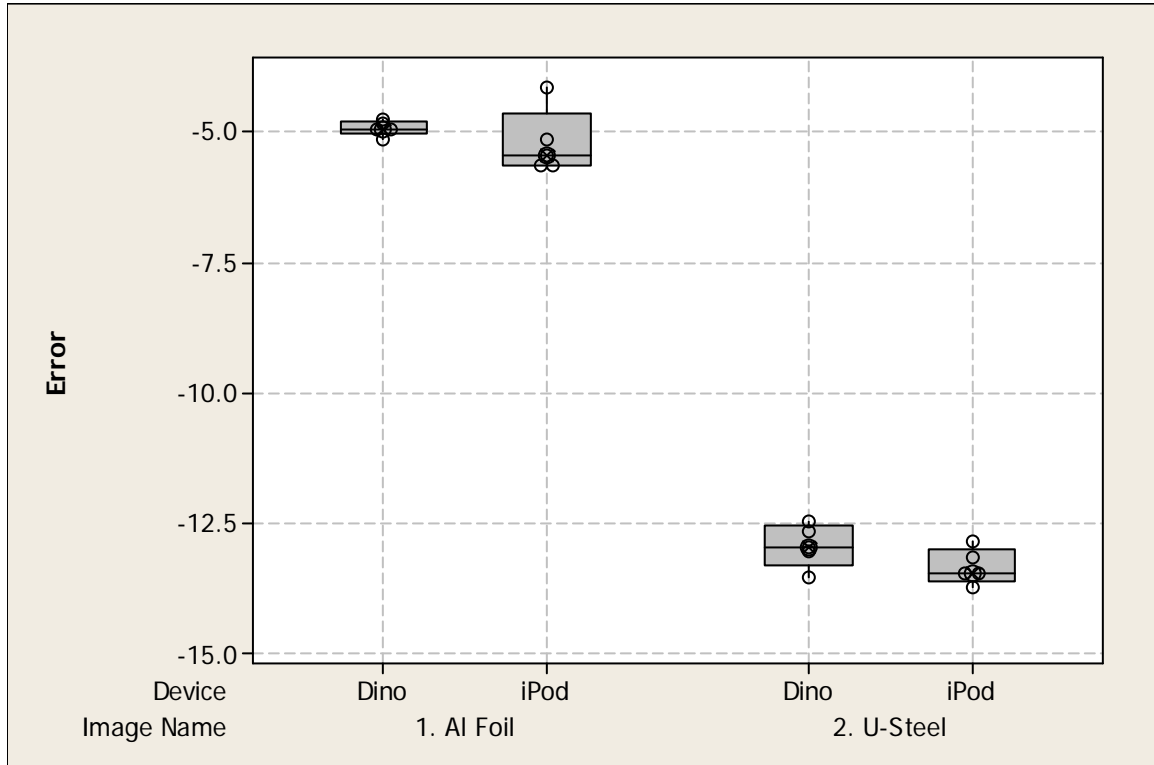
Figure 22. Boxplot of the Error in the Top-Down Method

Table 9, Data of the Error in the Top-Down Method

Device	Analysis Method	$\bar{x}$ (°)	s (°)	N
1. Al Foil	Dino	$-4._9$	0.1_5	5
	iPod	$-5._2$	0.6_3	5
2. U-Steel	Dino	$-12._9$	0.4_2	5
	iPod	$-13._3$	0.3_4	5

The last method investigated was the Langmuir method using the Contact-θ-Meter and the iPod with the Theodolite (*iPod*) application. Figure 23 shows the error in the two less than 90 degrees standards using the Contact-θ-Meter and the iPod.
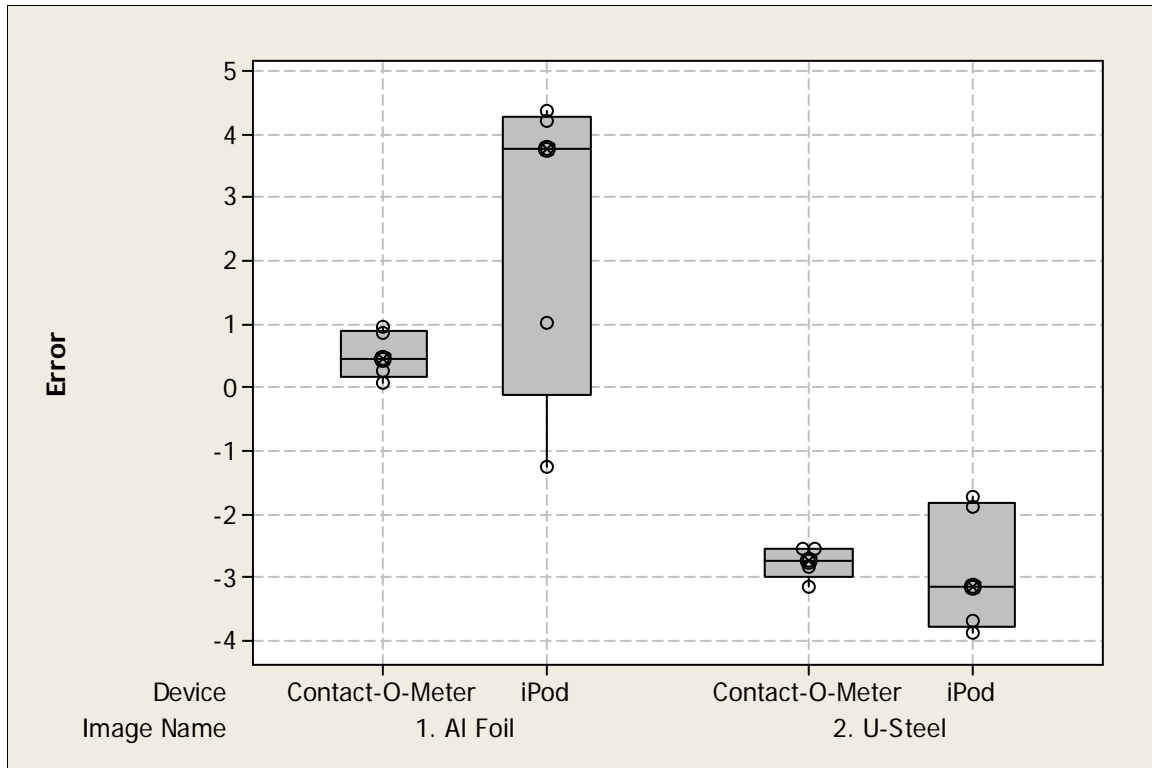
Figure 23. Boxplot of Error in the Langmuir Method

Table 10, Data of Error in the Langmuir Method

Device	Analysis Method	$\bar{x}$ (°)	s (°)	N
1. Al Foil	Contact-θ-Meter	$0._5$	0.3_8	5
	iPod	$2._4$	2.4_6	5
2. U-Steel	Contact-θ-Meter	$-2._8$	0.2_5	5
	iPod	$-2._9$	1.0_0	5

CHAPTER VI

DISCUSSION

The measurement of the contact angle of a liquid on a surface is related to wettability and surface energy information. The literature study confirmed that although many of the adaptations were primitive, three theories could be combined with improvements in digital imaging and computing to bring contact angle measurements to the modern coating or adhesive production facility. The three primary approaches to looking at a drop; the side-on (Young), top-down (Bikerman) and reflected angle (Langmuir) methods present their own challenges and advantages when measuring a drop. In order to effectively compare these methods, several standard reference materials were created.

The first step in the contact angle method comparisons was to determine the accepted contact angle for each of the standards. Table 1 described the mean contact angle for each of the standards as analyzed using the images taken using the side-on approach with the digital microscope and the contact angle calculated using the Manual Points Procedure. The calculations revealed, after five measurements, that the uncertainty in each of the measurements was very low. Goniometer measurements in industry typically have a resolution of between 0.01and 0.1 degrees for contact angle, while the measurements using the lab accepted technique has a resolution of between 0.3 and 0.6 degrees. [34, 35] Although the data collected here had lower resolution, it is still comparable to the goniometer.

The side-on, microscope, Manual Points Procedure analysis was chosen as this approach most closely relates to the lab practice goniometer methods. The Manual Points Procedure also has the advantage of the drop not needing to be level before analysis. Since the DinoLite microscope has the highest resolution and there are five points taken into account in analysis, the edge of the drop is clearly outlined by the user without needing to alter any threshold values allowing for optimum measurement of the tri-phase point. These values then can be used as the accepted lab standard for which all the methods will be compared.

Side-on Methods and Standards

Once the accepted contact angle was measured, the two approaches to the side-on method were analyzed. As Williams, *et al.,* [24] explained, the side-on method with the camera placed perpendicular to the drop works for contact angles of greater than or less than 90 degrees. Therefore, the first attempt of the side-on method was made to use a ruby ball mounted in a gage card to simulate a sessile drop. Both the ruby ball and the gage card on which it is mounted are well machined, giving a profile similar to a sessile drop. Unfortunately, due to the thickness of the gage card, the neither ball could be mounted in the gage card to mimic a contact angle of less than 90 degrees as Figure 24 illustrates. The left side shows a view of the ruby ball so that the gap between the ball and gage card can be seen while the right side shows how the ball was held in the gage card.
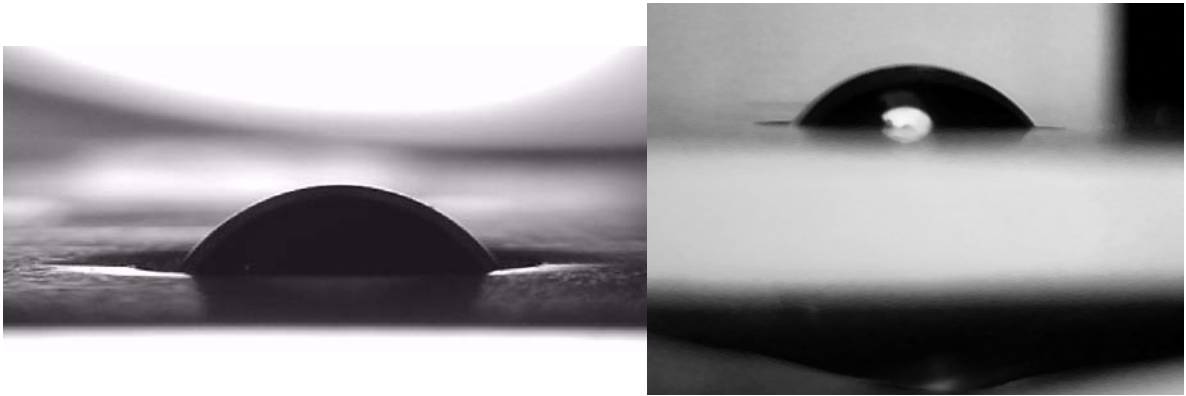
Figure 24. Ruby Ball in Gage Card at Less than 90 Degrees

The ball cannot provide a clear tri-phase point when mounted under the gage card as the gage card appeared to be far too thick for the under-mounting approach. The ruby ball was then only used for contact angles over 90 degrees. The half-angle and Brugnara methods were applied to the images of the ruby ball using the microscope with and without the mirror as well as with the iPod with the mirror. The prism was removed as a method because the prism did not provide a clear enough image for analysis as shown in Figure 25. There are rings present in the image that are internal reflections within the prism which cause cloudiness in the image.
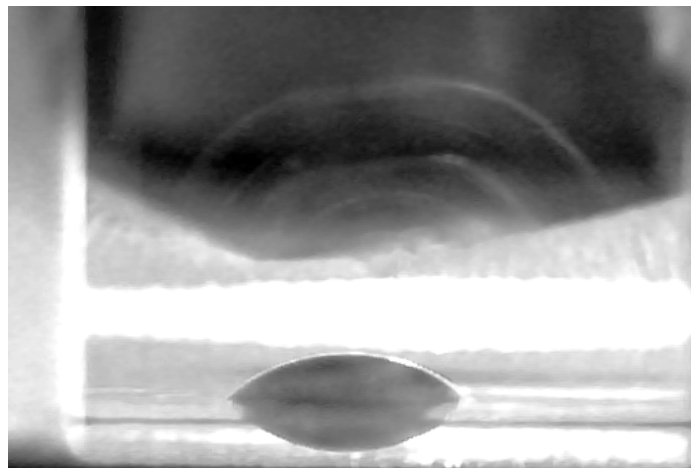
Figure 25. Example of Image Taken with the Prism

Specifications for the mirror and its placement were optimized here as well. The mirror used was a 15 mm by 15 mm highly polished piece of stainless steel bent 90 degrees to form the mirror, supplied by our colleague Dr. Anslem Kuhn in the United Kingdom. In regards to placement relative to the standard, the mirror was placed one inch from the edge of the standard. The microscope lens was 2.22 cm from the top of the drop while the iPod, with its 0.64 cm thick lens, was 4.13 cm away from the standard. These values were not optimized, but merely used to maintain consistency in this experiment. If the mirror was placed further away, or the microscope or iPod placed higher, then the distance from the standard would be increased causing less resolution in the image.

In Figure 20, the less than 90 degree standards measured with a mirror were about two degrees lower and the greater than 90 degree standards were measured almost four degrees lower. It is appropriate to differentiate between the systematic and random error seen throughout the data presented here. For example, the systematic error seen in Figure 20 lies with the fact that the mirror images produced contact angle values decisively lower than the zero point value. The random error laid within the variance among the image measurements since not all were low. The random error can most likely be attributed to the combination of the contact angles provided by the half-angle, Manual Points, and Circle Best Fit procedure being used during the analysis of the less than 90 degree standards and just the half-angle and Manual Points procedures in the greater than 90 degree standards. The systematic error can be attributed to either the analyst or the placement of the mirror. By improving measurement technique, the analyst's contribution could be removed. To correct for the mirror, an analysis of the attributes of the mirror including natural reflectance could be measured. Analyzing the attributes of the mirror

and optimizing its placement in relation to the standard and the iPod or microscope can also decrease the error seen in measuring the contact angle of the standards. Even checking into how much light is being added to the image by the mirror could help to alleviate any problems with contrast in the images. A simple screen eliminating the amount of light hitting the mirror and an optimized placement of the mirror could decrease both the systematic and random error seen in the analysis of the images taken using the mirror.

By replacing the gage card with a piece of a punched aluminum sheet, __ micrometers in thickness, the steel ball could mimic the less than 90 degrees contact angle with a more distinct tri-phase point. The images in Figure 26 illustrate the suggested approach. The thinner sheet of aluminum allows the small crevice created between the ball and gage card, as seen on the left in Figure 26, to be minimized. Figure 27 is an image of the steel ball in the piece of aluminum with a hole punched in it.

Ball Mounted on
Underside of Gage
Card

Ball Mounted on
Underside of Thin
Aluminum Sheet
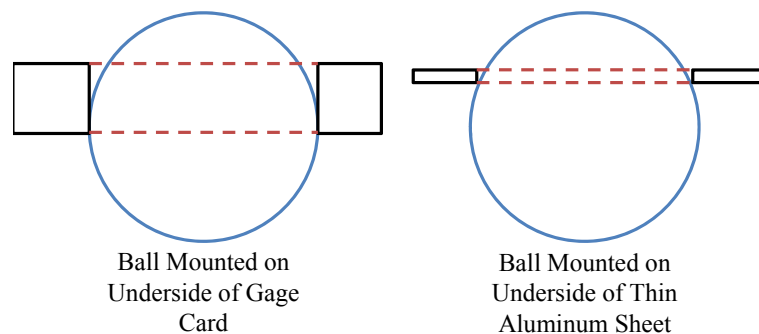
Figure 26. Comparison of the Gage Card and Punched Thin Aluminum Sheet
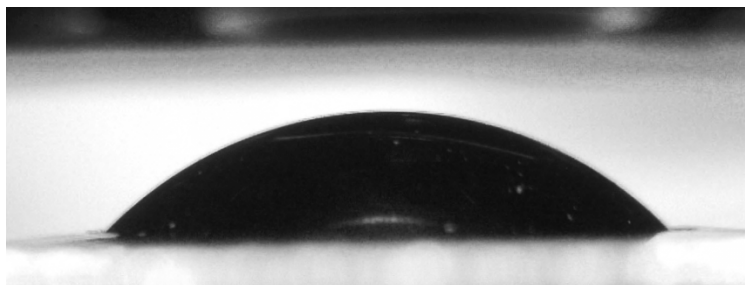
Figure 27. Under-mounted Steel Ball in Punched Aluminum

To try to improve on the punched aluminum, several attempts were made to mount the balls in a plastic. Mounting the ball in plastic would have allowed the creation of a rugged standard prototype. Table B1 in Appendix B shows the images of the attempts made. All of the attempts proved to be ineffective as the plastic either created a meniscus too far up on the ball or air pockets, both of which prevented a clear view of the tri-phase point.

The data from all four standards were analyzed using the images taken with the microscope, the microscope with the mirror, and the iPod with the mirror. Once the data was imported into MiniTab, Table 2 was generated to describe the error in the three different approaches to the side-on methods. The error calculations were done using the Manual Points Procedure and half-angle method for all four standards, while the less than 90 degree contact angle standards were also measured with the Circular Best Fit approach. The Circular Best Fit approach uses edge detection by the computer while the Manual Points Procedure uses the naked eye as the edge detector. The Circular Best Fit approach worked poorly on the images taken using the mirror, causing the higher variance seen in the contact angles measured in Table 2. The table suggests that even though the lab accepted value was the side-on method, the mirrors still had a high amount of variance.

The boxplot in Figure 15 compares all of the standards with all three measurement methods. The Brugnara Manual Points Procedure method was chosen as the preferred method for side-on analysis, and Figure 20 and Table 7 showed that the microscope without the mirror provided the lowest average error. By partitioning the data by standard, method, and technique, the analysis shows that the contact angle measurements are very dependent on the image analysis. The worst analysis method was with the iPod and mirror set-up on the under-mounted steel ball analyzed with the Circular Best Fit approach as described in Figure 17 and Table 4. When looking at the image, it was clear that the reflection on the edge of the ball made it too hard for the computer to see and appropriately measure the edge. The Manual Points approach allowed the analyst to pick the edge of the standard which removed the need for the threshold values and the possibility of the computer not recognizing the actual edge. Almost all of the other measurements lied within a five degree range above and below the zero point, which then became the accepted range of values to determine if an analysis method was done accurately. Those measurements that lie outside were taken using the mirror set-up as seen in Figure 20 and Table 7. Even though the direct side-on approach was the lab accepted standard, the mirror had too much variability in measurements, even though the majority lie within a 10 degree range as shown in Figure 16 through Figure 19 and Table 2 through Table 6.

In Table 3 and Figure 16, the pressed aluminum standard when measured using the iPod and mirror had a greater amount of random error no matter which analysis technique. Although the side-on approach with the Manual Points procedure was chosen as the lab accepted value, the mirror approach using the microscope had more precision

across all three analysis techniques, but the values were right around two degrees lower than the zero point. The under-mounted steel was difficult to analyze with the iPod as well, with the Circular Best Fit approach having an average error of 11 degrees from the zero point. The reason for this can be attributed to the computer being unable to accurately find the edge of the ball due to poor contrast. The side-on approach had the lowest deviation across all three analysis methods, with the mirror with the microscope not too far behind, as seen in Figure 17 and Table 4.

The data presented in Figure 18 and Table 5 outline that for the ruby ball both the mirror methods measured the contact angle right around five degrees lower than the zero point. The microscope also had the highest amount of random error in the contact angle measurements. Even though the side-on approach was the preferred method, the iPod had lower variance than the microscope without the mirror. Through analysis of the steel ball data as shown in Figure 19 and Table 6, it can be discerned that the steel ball needed better contrast for the images taken with the iPod and microscope with the mirror. The amount of variance, although under the five degree limit, was still rather large compared to the side-on approach.

All the analysis done on the images with the mirror and with the strict side-on approach asserted that the mirror accounted for some of the systematic error visible in the measurements. The systematic error can be attributed to the distance created from reflecting the image to the camera and the lighting on the standards that could have come from the mirror reflecting excess room light into the image. The excess light and distance were not explored in this study.

Since the lighting played a big role in the image quality, the lighting of the drop became one of the primary concerns when looking at the contact angle error. Figure 21 and Table 8 when analyzed confirmed that by using a screen to block light the problems with blurry edges in the images are eliminated. In some images, the tri-phase point was too unclear from shading caused by the gage card or aluminum that the standard was resting on or in. The unclear edges and tri-phase point prevent one from effectively being able to apply the drop shape analysis techniques to the images which make any measurement made likely to be high in error. The use of diffuse light from directly behind provided a much clearer image for the steel ball, aluminum, and ruby ball standards. The under-mounted steel ball standard showed almost no error dependency on the presence of a screen.

Top-Down Methods and Standards

Since the tri-phase point could not be used to measure the contact angle, the Bikerman method and Top-Down Calculator spreadsheet were applied. The methods require the placement of a calibration object in the image. In this study, a metal washer provided the calibration object. The internal circumference of the metal washer was measured with a caliper. This allowed a conversion between pixels and millimeters so that the volume of each standard could be calculated properly for use in Equation 3.

The initial images were taken with the digital microscope as done in the side-on methods. The Top-Down Calculator spreadsheet allows for the analysis of drops only when the volume is known. The second round of images used a cell phone camera rather than a microscope. The approach used in the Williams[25] paper was recreated using the ruby ball, steel ball and aluminum standard. With all three standards, the cell phone

cameras provided pictures that were of good enough quality to apply the Bikerman method and measure the contact angles.

Figure 22 showed that the top-down method had a higher error associated with it which was not brought on by the use of either device since in the boxplot both devices were very close in the angles measured, but were way off the zero line. The top-down method only worked well for the aluminum standard, it worked very poorly for the under-mounted steel ball. The aluminum standard was measured right around five degrees lower than the accepted value while the under-mounted steel ball was closer to 13 degrees lower. The five degrees of the aluminum standard is still consistent with the five degrees seen in the side-on approaches. The issue with the steel might be due to the ball not sitting perfectly flush with the punched aluminum which can create a gap that the Bikerman equation cannot account for. As stated previously, the average error among industry methods is between 0.01 and 0.1 degrees, so the top-down method had a very high variability as compared to the industry standard.

Reflected Angle Methods and Standards

In order to mimic the Contact-θ-Meter, a small fiber-optic light was used to highlight the drop in a similar fashion so the iPod could be used as the viewing tube. The Theodolite application measured the elevation of the iPod through focusing the optical center line of the camera on the tri-phase point facing the light. The application provided an elevation instantaneously, which must then be plugged into Equation 6 for φ, providing an excellent imitation of the Contact-θ-Meter.

Figure 23 demonstrated the error of the Contact-θ-Meter and the iPod. The reflection on the aluminum prevented a good analysis with the Contact-θ-Meter which

caused the higher contact angle measurements, even though all the measurements were still under the five degree error in the other methods. The iPod and the Contact-θ-Meter both analyzed the under-mounted steel ball a tad bit lower than the accepted contact angle value, but still were under the previously measured five degree error. The Contact-θ-Meter values were all very close to each other suggesting that the Contact-θ-Meter was more consistent than the iPod, but the iPod still was within the error range. The iPod and Contact-θ-Meter were very similar in error demonstrating that the iPod might be an acceptable substitute for the Contact-θ-Meter in the field.

Three standards showed promise as non-evaporating standards. The fragility of the aluminum foil prevents its use as a standard because the dome-shaped protrusion is easily dented. One improvement would be to pour liquid aluminum into some type of mold so that the low cost would be maintained, but the problems with deformability could be eliminated. The ruby ball would be a fair standard, but due to its higher cost it is not ideal for use in the field. The steel ball is a lower cost alternative to the ruby ball and does not show any problem with being used to mimic contact angles of greater than or less than 90 degrees. The preferred size for the steel ball is relative to the contact angle measurement required. The smaller the contact angle one wants to mimic, the smaller the size of the ball. A series of these balls could be mounted in such a way to mimic a variety of contact angles at one time with one type of standard. The main requirement is that the appropriate ball-hole combination be chosen to mimic theta.

CHAPTER VII

CONCLUSION

The use of contact angle measurement for surface energy is variable since the measurements themselves can vary greatly upon the choice of liquid placed on the surface and measurement technique. To alleviate some of this variability, a standard contact angle technique must be defined. Currently, a lab determines which technique is best suited for their purpose, and then picks the appropriate apparatus. Although attempts in the past had been made to generate some type of standardized method or apparatus [2-12], many are considered too primitive for widespread use or are too expensive for the average laboratory.

To reliably implement such a contact angle technique, there must be some way to determine if the technique is being used properly. At present, neither the National Institute of Standards and Technology nor the American Society for Testing and Materials has developed a calibration standard, and that makes it difficult to evaluate the accuracy of different measurement methods. The proposed non-evaporating contact angle standard would be suitable for use in the calibration of the apparatus and software.

In developing these standards, three methods of measuring the contact angle of the three proposed standards were compared. The methods tested here take root in those developed by T. Young [1], Irving Langmuir [13-14] and J. J. Bikerman [15]. The standards were a ruby ball mounted on a drill gage card, a piece of pressed aluminum foil, and a steel ball mounted on a drill gage card or under a thin sheet of aluminum. The aluminum foil was far too flexible and would need to be remade in such a way that it could not be

dented so easily before it could be used reliably in the field. The ruby ball, although highly spherical, was less cost effective than the other standards. For this study, the steel ball provided the highly spherical characteristics, was inexpensive, and able to mimic contact angles of less than and greater than 90 degrees making it the preferred choice of standard.

In evaluating the methods, the direct side-on method as defined by Young was the most closely related to current lab analysis techniques, so it was chosen as the lab accepted standard for contact angle measurement. The side-on method using a mirror increases uncertainty in contact angle measurement because of the increased distance of the camera from the standard made by the mirror increasing the uncertainty. The uncertainty is well within a five degree range, which is higher than the 0.01 to 0.1 degrees seen in industry apparatuses.

The top-down method as defined by Bikerman and the reflected angle method as defined by Langmuir were combined with the digital imaging and computing to provide better data analysis. The use of a camera phone and application provided a more accessible way for technicians to accurately and precisely measure droplets of any contact angle without the need for a stage or any other apparatus than a light source. The data revealed that the iPod is useful for field testing, providing a less than five degree error for most methods. The preferred method still lies with the digital microscope using the direct side-on approach. All in all, each of these methods presented unique challenges and advantages, but were effective at measuring wide ranges of contact angles.

The entire system combines known, inexpensive contact angle measurement techniques, with a non-evaporating standard that is undisturbed by the environment.

These are practical techniques that are suitable for field work or work involving large surfaces such as in the modern coating or adhesion production facility. Whether it is the side-on, top-down, or reflected angle method, the standards presented here each have their own advantages and disadvantages. The preferred standard is the steel ball as it can mimic both the less than 90 degree and greater than 90 degree contact angles by mounting it above or below a punched-metal sheet. Further work is needed to generate a complete working standard that could be marketed and is compatible with the inexpensive methods evaluated in this study. These standards are also compatible with many of the available commercial contact angle instruments.

BIBLIOGRAPHY

1. Young, T. An Essay on the Cohesion of Fluids. *Phil. Trans. R. Soc. Lond.* **1805,** *95,* 65-87.

2. Barth, J. J.; Zvan, G. R. Dynamic Contact Angle Measurement System. US 5143744, September 1, 1992.

3. Sutton, S. P. Capillary Devices for Determination of Surface Characteristics and Contact Angles and Methods for Using the Same. US 7024921 B2, April 11, 2006.

4. Sutton, S. P. Capillary Devices for Determination of Surface Characteristics and Contact Angles and Methods for Using Same. US 7308822 B2, December 18, 2007.

5. Blitshteyn, M.; Hansen, J.; Shaw, R. K. Method and Apparatus for Determining the Contact Angle of Liquid Droplets on Curved Substrate Surfaces. US 5137352 A, August 11, 1992.

6. Friedrich, B.; Frerichs, J.-G.; Kortz, E. Methods and Device for Contact Angle Determination from Radius of Curvature of Drop by Optical Distance Measurement. US 7952698 B2, May 31, 2011.

7. Wright, R.; Blitshteyn, M. Method and Apparatus for Measuring Contact Angles of Liquid Droplets on Substrate Surfaces. US 5268733, December 7, 1993.

8. Dumoulin, C. A.; Ausserre, D.; Rondelez, F. Method and Apparatus for Determining the Contact Angle of a Drop of Liquid Placed on a Solid or Liquid Horizontal Substrate. US 4688938, August 25, 1987.

9. Martin, P.; Le Bondee, G. Methods and Devices for Determining the Contact Angle

of a Drop of Liquid Placed on a Substrate. US 5115677, May 26, 1992.

10. Schneider, H.; Rinck, H. Method of Measuring the Contact Angle of Wetting Liquid on a Solid Surface. US 5080484, January 14, 1992.

11. Poppe, W.; Khelghatian, H. M. Contact Angle Measurement of Plastic Surfaces. US 3696665, October 10, 1972.

12. Wapner, P. G.; Hoffman, W. P. Liquid to Solid Angle of Contact Measurement. US 6867854 B1, March 15, 2005.

13. Livereel. *Contact-θ-Meter;* Pearson Panke Equipment Ltd: London.

14. Langmuir, I. The Constitution and Fundamental Properties of Solids and Liquids. II. Liquids. *J. Am. Chem. Soc.* **1917,** *39* (9), 1848-1906.

15. Bikerman, J. J. A Method of Measuring Contact Angles. *Industrial and Engineering Chemistry* **1941,** *13* (6), 443-444.

16. ASTM D7490 - 08 Standard Test Method for Measurement of the Surface Tension of Solid Coatings, Substrates and Pigments using Contact Angle Measurements, 2008. http://www.astm.org/Standards/D7490.htm (accessed Sept 24, 2011).

17. ASTM D7334 - 08 Standard Practice for Surface Wettability of Coatings, Substrates and Pigments by Advancing Contact Angle Measurement, 2008. http://www.astm.org/Standards/D7334.htm (accessed Sept 24, 2011).

18. Adamson, A. W.; Gast, A. P. *Physical Chemistry of Surfaces,* 6th ed.; Wiley Interscience: New York, 1997.

19. Ellison, A. H.; Zisman, W. A. Wettability Studies of Nylon, Polyethylene

Terephthalate, and Polystyrene. *The Journal of Physical Chemistry* **1954,** *58* (6), 503-506.

20. du Nouy, P. L. An Interfacial Tensiometer for Universal Use. *Journal of General Physiology* **1925,** *7* (5), 625-631.

21. Harkins, W. D.; Jordan, H. F. A Method for the Determination of Surface and Interfacial Tension from the Maximum Pull on a Ring. *J. Am. Chem. Soc.* **1930,** *52,* 1751.

22. Huh, C.; Mason, S. G. A Rigorous Theory of Ring Tensiometry. *Colloid Polymer Science* **1975,** *253,* 566-580.

23. Williams, D. L.; Jupe, C. L.; Kuklenz, K. D.; Flaherty, T. J. An Inexpensive, Digital Instrument for Surface Tension, Interfacial Tension, and Density Determination. *Ind. Eng. Chem. Res,* **2008,** *47,* 4286-4289.

24. Williams, D. L.; Kuhn, A. T.; Amann, M. A.; Hausinger, M. B.; Konarik, M. M.; Nesselrode, E. I. Computerised Measurement of Contact Angle. *Galvanotechnik* **2010,** *108* (11), 2502-2512.

25. Williams, D. L.; Kuhn, A. T.; O'Bryon, T.; Konarik, M.; Huskey, J. Contact Angle Measurements Using Cell Phone Cameras to Implement the Bikerman Method. *Galvanotechnik* **2011,** *109* (8), 1718-1725.

26. Williams, D. W. A Training Case Study in Repeatability and Reproducability. *PCx Cleaning Conference,* April 20, 2011.

27. *MiniTab,* 14th ed.; MiniTab Inc.: State College, PA, 2010.

28. Brugnara, M. *Contact Angle Plugin;* University of Trento: Trento Italy, 2010.

29. Rasband, W. S. *ImageJ;* U. S. National Institutes of Health: Bethesda, Maryland, USA, 2010.

30. Deriche, R. Using Canny's Criteria to Derive a Recursively Implemented Optimal Edge Detector. *Int. J. Computer Vision* **1987,** *1,* 167-187.

31. Roberts, B. *Meazure Ver. 2.0 Build 158;* C-Thing Software, 2004.

32. Langmuir, I.; Schaefer, V. J. The Effect of Dissolved Salts on Insoluble Monolayers. *J. Am. Chem. Soc.* **1937,** *59,* 2400-2414.

33. Hunter, C. A. *Theodolite;* Hunter Research and Technology LLC, 2012.

34. Kruss. Kruss: Advancing Surface Science. http://www.kruss.de/en/products/contact-angle/drop-shape-analysis-system-dsa25.html (accessed June 30, 2012).

35. Ramé-hart Instrument Co. Ramé-hart Contact Angle Goniometers and Tensiometers. http://www.ramehart.com/260.htm (accessed June 30, 2012).

APPENDIX A: GLOSSARY OF TERMS

Word/Phrase	Definition /Explanation
Base Contact Diameter	The diameter of the cicular contact area between a drop and a surface (*b*).
Bikerman Equations	$$\frac{b^3}{v} = \frac{24sin^3\theta}{\pi\,(2 - 3cos\theta + cos^3\theta)} \quad and \quad \frac{d^3}{v} = \frac{24}{\pi\,(2 - 3cos\theta + cos^3\theta)}$$ The equation relates the drop's base contact diameter, *b*, its volume, *v*, and the contact angle, *θ,* the drop forms with the surface. The equation requires that the drop be spherical, and this restricts the volume of the drops to within the microliter range. The first equation uses the base contact diameter (*b*) of the drop such that *θ* is less than 90 degrees, where the second uses the diameter (*d*) of the drop such that *θ* is greater than 90 degrees.
Brugnara method	A method using the Contact Angle plugin in the ImageJ program to define five points along the edge of the drop then a circle (Circle Best Fit), ellipse (Ellipse Best Fit), or the Manual Points Procedure is used to compare the contact angle of the drop.
Contact Angle	The angle of the tangent of the drop curvature with solid-liquid interface at the tri-phase point when the drop is viewed in profile.

Word/Phrase	Definition /Explanation
Critical Surface Tension	Any liquid with a surface tension less than the value will completely wet the surface in question. Reported in dynes per centimeter and labeled as γ_c.
Half-Angle Method	$$\theta = 2tan^{-1}\left(\frac{2h}{b}\right)$$ Measurement method that is only appropriate for perfect spheres in which the contact angle θ is the same no matter which way the drop is viewed.
Sessile Drop	A drop at rest on top of a surface.
Surface Energy	The amount of energy required to create a certain area of surface, reported in joules per meter squared.
Surface Tension	The surface energy of a liquid that it is expressed as a force in one dimension reported in newtons per meter.
Tri-Phase Point	The solid-liquid-air interaction point.

Word/Phrase	Definition /Explanation
Young's Equation	$$\gamma_{13} = \gamma_{12} + \gamma_{23} \cos \theta$$ Young's equation states that the surface tension between the solid/gas interface is equal to the surface tension at the solid/liquid interface plus the surface tension of the liquid/gas interface multiplied by the cosine of the contact angle the liquid makes with the solid.
Zisman Plot	A plot of the cosine of the contact angles of a series of liquids on a surface versus the known surface tensions of the liquids.

APPENDIX B: STEEL BALL ATTEMPTED STANDARDS

Since one of the key points of this study was to produce robust standards for use in the field, an attempt was made to mount the steel balls in some type of plastic so that it could mimic any contact angle just by varying the depth. These attempts did not yield any workable standard as the following table describes.
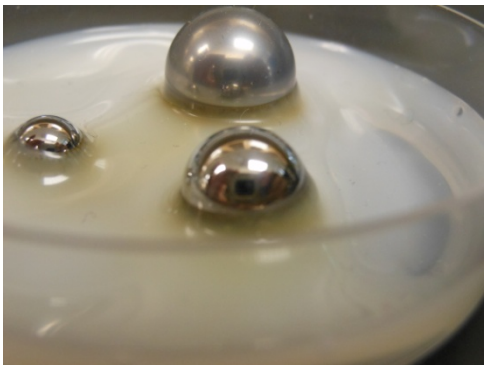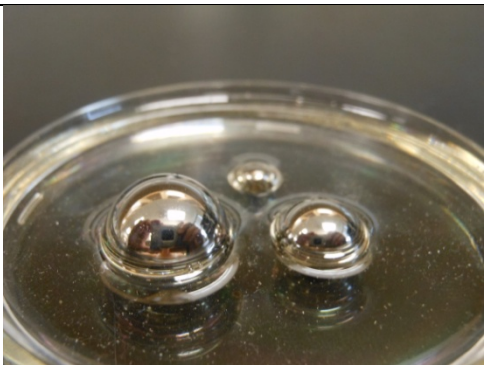
Table B1, Steel Ball Attempted Standards

Adhesive	Photograph	Description
Elmer's Glue		The glue, due to its high water content showed excessive shrink on cure, rusted the balls and could not provide a uniform seal around the ball. The glue either created too high of a meniscus on the ball or left a hole on the side.
Epon 828/ Versamid 140		The Epon/Versamid mixture does not provide a clear tri-phase point. The epoxy adhered to the side of the ball obscuring the tri-phase point for contact angle measurement.

Table B1, Steel Ball Attempted Standards Continued

Epoxy	Photographs	Description
Quick-Set Epoxy		The nature of the quick set epoxy prevented the ball from sinking into the epoxy.

APPENDIX C: VOLUME OF A SPHERICAL CAP DERIVATION

The volume of a spherical cap derivation is credited to Dr. Benny Arney of the Sam Houston State University Department of Chemistry. Figure C1 describes the relationship of the values as defined in the derivation below:
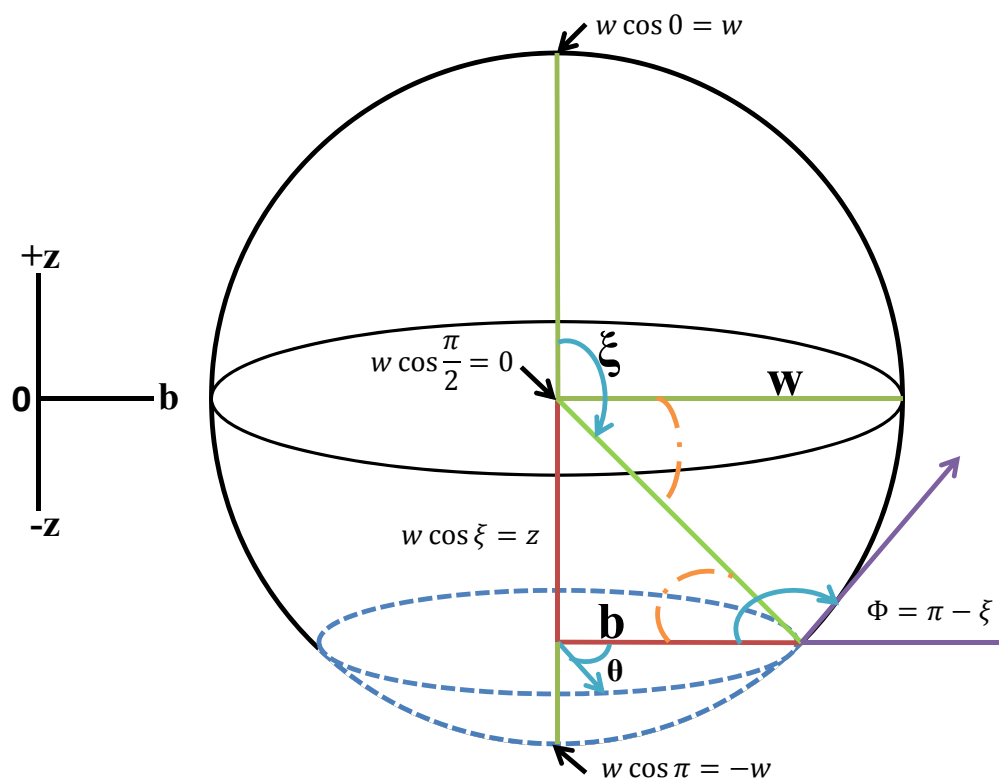

Figure C1. Volume of a Spherical Cap Derivation

The origin of the sphere is set at 0 on a polar coordinate system. Using polar coordinates, θ ranges from 0 to 2π while the radius of the drop w goes from 0 to $\sqrt{w^2 - z^2}$. At contact angles of greater than 90 degrees, the radius of the drop can be defined in terms of the waist of the drop. The waist of the drop is defined as the widest portion of the drop parallel to the surface the drop is resting on. The waist is more

commonly named the diameter; therefore based on Figure C1 two times w equals the

diameter D. At contact angles of less than 90 degrees, the radius of the drop can be

defined in terms of the base diameter of the drop. The base diameter of the drop is

defined as diameter of the circle that is created by the drop at the contact surface. In

Figure C1, two times b equals the base contact diameter B.

Now that the diameter, radius, and base contact diameter are defined, the height of

the drop must also be defined. When the contact angle is greater than 90 degrees, the

height is equal to the radius plus the height of the drop just from the origin to the surface

the drop is resting on. The height from the origin is labeled $z+(-z')$. z is also defined as

the height when the contact angle is less than 90 degrees.

At this point it is important to define the contact angle of the drop ξ. In order to

calculate the contact angle, the radius, waist, and base contact diameter are related to the

contact angle. The following equations apply:

$$z = w \cos \xi \ \ and \ \ b = w \sin \xi \ \ therefore \ \ \sin \xi = \frac{b}{w}$$

As the height of the drop z moves from 0 to $2w$, the relationship to the contact

angle is a simple cosine function. As the base diameter changes, the relationship to the

contact angle is a simple sine function. Therefore, for a sphere with a radius of w,

truncated at $z = w \cos \xi$ in the polar coordinate system, the following integration can be

made.

$$V = \int_0^{2\pi} \int_{w \cos \xi}^{w} \int_0^{\sqrt{w^2 - z^2}} r \, dr \, dz \, d\theta = 2\pi \int_{w \cos \xi}^{w} \int_0^{\sqrt{w^2 - z^2}} r \, dr \, dz$$

The integration for θ is a solid of rotation integration which gives the 2π term.

$$= 2\pi \int_{w\cos\xi}^{w} \left(\frac{r^2}{2}\right)\Big|_0^{\sqrt{w^2-z^2}} dz = \pi \int_{w\cos\xi}^{w} (w^2 + z^2)dz$$

After simplifying the integration of the r term:

$$= \pi \left(w^2 z - \frac{z^3}{3}\right)\Big|_{w\cos\xi}^{w} = \pi \left(w^3 - \frac{w^3}{3} - w^3 \cos\xi + \frac{w^3 \cos^3\xi}{3}\right)$$

Making the argument that the diameter D is equal to $2w$, the following

substitution and simplification can be made:

$$V = \pi w^3 \left(\frac{2 - 3\cos\xi + \cos^3\xi}{3}\right) = \pi D^3 \left(\frac{2 - 3\cos\xi + \cos^3\xi}{24}\right)$$

$$\frac{D^3}{V} = \frac{24}{\pi(2 - 3\cos\xi + \cos^3\xi)}$$

Using the equation $\sin\xi = \frac{b}{w}$, a substitution of D can be made.

$$V = \pi \left(\frac{b}{\sin\xi}\right)^3 \left(\frac{2 - 3\cos\xi + \cos^3\xi}{3}\right) = \pi \left(\frac{B}{\sin\xi}\right)^3 \left(\frac{2 - 3\cos\xi + \cos^3\xi}{24}\right)$$

$$\frac{B^3}{V} = \frac{24\sin^3\xi}{\pi(2 - 3\cos\xi + \cos^3\xi)}$$

$$\frac{B^3}{D^3} = \sin^3\xi$$

In the end, the derivation shows that the Bikerman equation can be used with both

the diameter and the base contact diameter as long as a conversion is made. The

conversion is inherent in the sine cubed term, which is essential in the Top-Down

Calculator.

VITA

Trisha Marie O'Bryon

Home Address   1712 Spanish Trail
                       Plano, TX 75023

EDUCATION

Master of Science in Chemistry at Sam Houston State University, August 2010 – present.

Bachelor of Science (May 2010) in Chemistry, Sam Houston State University, Huntsville, TX.

ACADEMIC EMPLOYMENT

Graduate Teaching Assistant, Department of Chemistry, Sam Houston State University, August 2010 to May 2012. Responsibilities include: the instruction and preparation of materials for chemistry majors in Quantitative Analysis, Organic Chemistry, and Physical Chemistry.

Research Assistant to Dr. Darren L. Williams, Department of Chemistry, Sam Houston State University, May 2009 to present. Research responsibilities include: researching the preparation of a non-evaporating contact angle standard reference material, the miscibility of solvents using enthalpy and entropy of mixing equations, and the use of Hansen Solubility Parameters to remove adhesives from metal surfaces for use by the Department of Energy at B&W Pantex in Amarillo, TX.

Undergraduate Teaching Assistant, Department of Chemistry, Sam Houston State University, January 2008 to 2010. Responsibilities include: the instruction in general laboratory techniques for non-major chemistry students in the Introduction to Inorganic and Environmental Chemistry, and the Introduction to Organic and Biological Chemistry.

PUBLICATIONS

Williams, D. L.; Kuhn, A.; O'Bryon, T.; Konarik, M.; Huskey, J. Contact Angle Measurements Using Cell Phone Cameras to Implement the Bikerman Method. *Galvanotechnik* **2011,** *109* (8), 1718-1725

PRESENTATIONS AT PROFESSIONAL MEETINGS

O'Bryon, T. M., and Darren Williams. Contact Angle Measurements for Cleanliness Verification. 1st Annual US Department of Energy Partnering in Technology Conference, West Texas A&M University, Canyon, Texas, April 22nd, 2010.

ACADEMIC AWARDS

Dean's List at Sam Houston State University from 2007-2008 and 2009-2010

Department of Chemistry scholarships at Sam Houston State University in 2007-2010

National Merit Scholarship from Lennox Industries from 2006-2010

National Society of Leadership and Success Former Advisory Board Member in 2012-2013

Robert A. Welch Research Scholarship Recipient at Sam Houston State University in 2009, 2011 and 2012

Who's Who Among American Colleges and Universities from 2008-2010

PROFESSIONAL MEMBERSHIPS

American Chemical Society

Elliot T. Bowers Honors College Alumni

Phi Alpha Theta

Sigma Delta Pi

The National Society of Leadership and Success (Sigma Alpha Pi)